IS THERE AN ASSOCIATION BETWEEN FRONTAL FIBROSING ALOPECIA AND SUNSCREEN ACTIVES?

by

KUTLWANO ANTONETTE CHABAESELE

CHBKUT001

SUBMITTED TO THE UNIVERSITY OF CAPE TOWN

In fulfilment of the requirements for the degree

MSc Trichology and Cosmetics Sciences

Faculty of Health Sciences

UNIVERSITY OF CAPE TOWN

February 2019

Supervisor:

DR H.A ADEOLA (University of Cape Town, Department of Medicine)

Co-supervisor (s):

PROF N.P KHUMALO (University of Cape Town, Department of Medicine)

DR M.R LEBEKO (University of Cape Town, Department of Medicine)

DECLARATION

I, Kutlwano Chabaesele, hereby declare that the work on which this dissertation/thesis is based is my original work (except where acknowledgements indicate otherwise) and that neither the whole work nor any part of it has been, is being or is to be submitted for another degree in this or any other university.

I empower the university to reproduce for research either the whole or any portion of the contents in any manner whatsoever.

Signature: …Signed by candidate

Date: 11 February 2019

ABSTRACT

Background

Frontal fibrosing alopecia (FFA) is a subtype of primary scarring alopecia. It is associated with progressive, lymphocytic inflammation of hair follicles and permanent replacement by fibrous tissue. Clinically FFA is characterized by a band-like recession of the frontal hairline which may be associated with eyebrow (+/- body hair) loss and facial hyperpigmentation (most significant in pigmented skin). Early reports of FFA were in a few postmenopausal women, however, there has been an exponential increase in published cases (which include young women and men) in the last decade. Even though the cause remains unknown, an environmental factor is suspected.

Aim

The main aim of the study was to investigate whether there is an association between FFA and sunscreen actives, and to compare this with a histologically similar condition (lichen planopilaris - LPP) and another which also affects the marginal scalp (Traction alopecia – TA). The objectives were to obtain archival pathology tissue collected in the last decade from scalp biopsies and to use high-end spectroscopy and microscopy to detect the presence of sunscreen actives. Secondly, to investigate the survival and metabolism of cultured skin cells after exposure to various sunscreen actives.

Methods

The presence of sunscreen actives in formalin fixed paraffin-embedded (FFPE) punch biopsies of 9 FFA, 11 LLP and 5 TA, were compared. Tissue sections (5 µM) were embedded on microscopy glass slides and analysed using a scanning electron microscope (SEM). Elemental analysis of the biopsies sections was carried out using the energy dispersive X-ray microanalysis/spectroscopy (EDS) function on the SEM. In addition,

Fourier-Transformed Infrared (FTIR) spectroscopy, was used to identify chemical bonds within biopsies, to potentially expose their molecular detail. The results were analysed using multivariate analysis known as Orthogonal Partial Least Squares Discriminant Analysis (OPLS-DA).

Secondly, immortalized human keratinocytes (HaCaTs) as well as fibroblasts derived from FFA site specific biopsies (normal scalp, active edge and scarred area) from 4 FFA patients were exposed to 5 common sunscreen actives *viz*: titanium dioxide, zinc oxide, octyl methoxycinnamate, benzophenone-4 and 2-ethylhexyl dimethyl PABA, over a 24 hrs period. Thereafter, cell counting kit-8 (CCK8) assay was used to measure the cytotoxicity effect of the 5 sunscreen actives on HaCaTs and primary fibroblasts. Further, the metabolic phenotype switch of treated cells was analysed using the real-time extracellular flux bioanalyser.

Results

SEM/EDS - various elements were detected in patients' biopsies, many seemed to be lower in FFA compared to LLP and TA samples such as potassium, promethium, terbium, thulium and tin. Bromine, chlorine and indium were unique to TA samples; lead was only found in 2 LPP samples and 3 elements (antimony, plutonium and arsenic) were only unique to FFA samples. Zinc was detected in more FFA (33%) than LPP (9%) and TA (0%) samples.

FTIR – various compounds were found in the FFPE sections. Strontium titanate was a significant contributor to the spectra separating FFA from TA; and although present was not significant for separating LPP vs. FFA and LPP vs. TA. Strotium titanate is used as a diamond simulant and one of the compounds it is produced from is titanium dioxide. Its use in jewellery makes it highly possible for it to come into contact with human skin. Moreover, there was no significant data point separation between FFA and LPP (R2 =55%), however, the R2 for FFA vs. TA and LPP vs. TA were 92% and 93% respectively and this shows that

there was a good separation of data points between two groups comparison. Three compounds strontium titanate, potassium phosphate tribasic which is used as a food additive and 1,2-Dichloroethylene which is used in cleaning applications of electronics and metals, were found to be significant contributors for the separation of data points between FFA vs. TA. Whereas, molybdenum iodide anhydrous (a compound used for research purposes in optical phenomena) and sodium metaperiodate (used in fluorescent labelling) were responsible for the separation between LPP vs. TA.

CCK8 - The human keratinocyte cell line and FFA primary fibroblasts showed varying susceptibility to sunscreen actives, with zinc oxide being most cytotoxic.

Real-time extracellular flux analysis - zinc oxide induced an aerobic phenotype switch only on keratinocytes. Titanium dioxide induced an energetic phenotype switch in both cell types, but increasingly more in fibroblasts from FFA active edge and scar samples. Chemical sunscreen actives showed negligible effect on the energy phenotype of both cell types.

Conclusion: Consistent with current clinical understanding, this proof-of-concept study found no significant FTIR spectra separation between FFA and LPP. However, strotium titanate (with source as titanium dioxide) may be a contributor to FFA pathogenesis. More FFPE samples from FFA patients had traces of zinc than those from LPP and TA. Further, zinc oxide proved to be the most cytotoxic and titanium dioxide to exhibit significant bioenergetic changes compared to chemical sunscreen actives on mono-layer cells (from a keratinocyte cell line and patient derived fibroblasts). The effect of physical sunscreen actives (traditional and nano-particles) warrants further investigations on more complex (closer-to-real-life) 3D in vitro and ex vivo FFA tissue culture models. Furthermore, investigating a larger cohort could improve identification of the link between sunscreen products and the development of FFA.

ACKNOWLEDEMENTS

First, I would like to thank the Heavenly Father for giving me the courage and strength in accomplishing my work.

I would also like to honour and thank my supervisors Dr H.A Adeola, Prof. N.P Khumalo and Dr M.R Lebeko for their continuous remarkable support and guidance they granted me throughout my project. A special gratitude to Prof. Khumalo for seeing potential in me and granting me the opportunity to be part of the great Hair and Skin Research (HSR) lab. Not forgetting my incredible lab colleagues from HSR lab, who offered me moral support and assistance with my lab work, whenever I needed an extra helping hand; and everyone who gave me their support throughout my project including my dearest family.

Also, big appreciation to my BSc (Hons) supervisor Prof Emmanuel Mukwevho, who pushed me out of my comfort zone and made me realize my full potential by advising me to join the UCT family. Not forgetting the incredible Agano Kiravu and Shameem Jaumdally, whom helped me a great deal with organizing my data, making it more presentable together with its statistics. I would like to extend my sincere gratitude to the National Research Foundation (NRF) for their financial support of this project and to the Mayosi Group Scholarship for the postgraduate research bursary they provided me with, to ensure that I finish my research project.

All this would have not been possible, without your incredible overwhelming support.

Table of Contents

LIST OF FIGURES

LIST OF TABLES

ABBREVIATIONS

ATR: Attenuated Total Reflection

CCK8: Cell Counting Kit 8

CD 8^+ T: Cytotoxicity T Cells

CO_2: Carbon Dioxide

DHEA: Dehydroepiandrosterone

DMEM: Dulbecco's Modified Eagle Medium

DNA: Deoxyribonucleic Acid

EDS: Energy Dispersive X-Ray Spectroscopy

FCCP: carbonilcyanide p-(trifluoromethoxy)phenyl-hydrazone

FDA: Food Drug Association

FFA: Frontal Fibrosing Alopecia

FBS: Fetal Bovine Serum

FFPE: Formalin Fixed Paraffin-Embedded

FTIR: Fourier-Transform Infrared

HaCats: Immortalized Human Keratinocytes

HFSC: Hair Follicle Stem Cells

HPF: Human Primary Fibroblast

HREC: Human Research Ethics Committee

LC: Langerhans Cells

LDH: Lactate Dehydrogenase

LPP: Lichen Planopilaris

MTS: 3-(4,5-dimethylthiazol-2-yl)-5-(3-carboxymethoxyphenyl)-2-(4-sulfophenyl)-2H-tetrazolium

MTT: 3-(4,5-dimethylthiazol-2-yl)-2,5-diphenyltetrazolium bromide) tetrazolium

NHLS: National Health Laboratory Service

OPLS-DA: Orthogonal Partial Least Squares Discriminant Analysis

PABA: Para-aminobenzoic acid

PCA: Primary Cicatricial Alopecia

PDF: Patient Derived Fibroblasts

PPAR: Peroxisome Proliferator-Activated Receptor

P/S: Penicillin and Streptomycin

ROS: Reactive Oxygen Species

SEM: Scanning Electron Microscope

SLS: Sodium Lauryl Sulfate

SIMCA: Software Independent Modelling of Class Analogy

SPF: Sun Protection Factor

TA: Traction Alopecia

TGBβ1: Transforming Growth Factor B

TO_2: Titanium Dioxide

UV: Ultraviolet

WST-1: 2-(4-iodophenyl)-3-(4-nitrophenyl)-5-(2,4-disulfophenyl)-2H-tetrazolium

XF: Extracellular Flux

XTT: 2,3-bis(2-methoxy-4-nitro-5-sulphophenyl)-5-carboxanilide-2H-tetrazolium

ZnO: Zinc Oxide

DEFINITIONS

FFA edge - area of the scalp where the hair regression it is still actively ongoing

FFA scar – area of the scalp where the hair has already been lost and hair follicles are replaced by fibrous tissue

CHAPTER 1

1. INTRODUCTION

1.1 INTRODUCTION AND LITERATURE REVIEW

Hair plays a significant psychological role in mammals, particularly in humans (1). Socially, it contributes to self-esteem in many individuals, as demonstrated by trendy hairstyles (2). Human hair also plays important physiological roles such as trapping airborne particles in sensitive areas like nasal and ear canals. Hair is mostly composed of proteins like keratins, and it is produced in a structure called the hair follicle. The hair follicle contains the hair bulb and hair bulge, which contain a variety of living cells found to be responsible for the ongoing production and pigmentation of the hair shaft (1&3). These include cells such as epithelial stem hair follicle cells, keratinocytes, melanocytes and mesenchymal cells (1). The hair biology cycle consists of three continuous stages - anagen, catagen and telogen (1). Anagen is the active growth phase, it is the longest stage of the hair cycle and may last up to 6 years (3). The catagen phase is the regression phase, which begins at the end of the anagen phase. In this phase differentiation of various hair cells is halted and the lower half of the follicle moves closer to the surface (4). Finally, telogen is the resting phase, where hair follicle remain dormant until the hair shaft is shed and makes way for the newly generated hair follicle (4). Any changes or disruption to this physiological cycle, could either result in conditions such as a complete loss of hair or a slowed hair growth rate (3).

Considering its important social and psychological functions in humans (2), hair needs to be well taken care of. Tanus, Oliveira (5) reported that many women and men (seldom) across the globe are highly concerned with the aesthetics of their hair, and this often leads them to follow the hair straightening, growing and dyeing trends, using various techniques,

including chemical hair products (5&6). The danger of following such trends is potential hair loss disorders, such as traction alopecia (5&7).

Hair loss (alopecia) can affect both men and women and can occur because of both extrinsic and intrinsic factors. It is usually classified into two forms, namely scarring and non-scarring alopecia (8). The scarring form mainly involves permanent hair loss, whereas non-scarring alopecia is potentially reversible (8).

Scarring alopecia can be further subdivided into two categories; primary and secondary cicatricial alopecia (8). Primary scarring alopecia (PCA) is believed to be initiated by inflammatory cells such as lymphocytes and polymorphs like neutrophils (9). This inflammatory reaction is believed to lead to a permanent destruction of the hair follicle (10). The exact pathogenesis of the inflammatory reaction in PCA is yet to be fully elucidated (10). However, the current classification of PCAs is based on predominant inflammatory cells (Figure *1*).

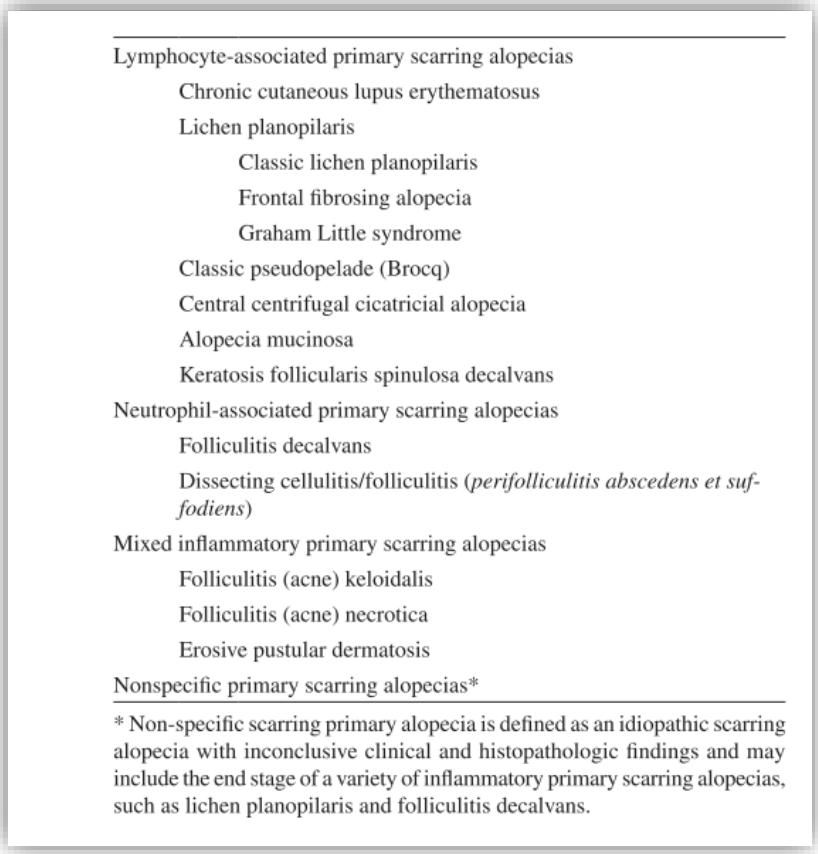

Lymphocyte-associated primary scarring alopecias
Chronic cutaneous lupus erythematosus
Lichen planopilaris
Classic lichen planopilaris
Frontal fibrosing alopecia
Graham Little syndrome
Classic pseudopelade (Brocq)
Central centrifugal cicatricial alopecia
Alopecia mucinosa
Keratosis follicularis spinulosa decalvans
Neutrophil-associated primary scarring alopecias
Folliculitis decalvans
Dissecting cellulitis/folliculitis (*perifolliculitis abscedens et suffodiens*)
Mixed inflammatory primary scarring alopecias
Folliculitis (acne) keloidalis
Folliculitis (acne) necrotica
Erosive pustular dermatosis
Nonspecific primary scarring alopecias*

* Non-specific scarring primary alopecia is defined as an idiopathic scarring alopecia with inconclusive clinical and histopathologic findings and may include the end stage of a variety of inflammatory primary scarring alopecias, such as lichen planopilaris and folliculitis decalvans.

Figure 1 Classification of PCAs according to the North American Hair Research Society (11).

Secondary scarring alopecia may be initiated by extrinsic factors such as trauma, infections and burns (12). In this study, the focus is on a subtype of PCA namely frontal fibrosing alopecia (FFA).

FFA is a subtype of primary cicatricial alopecia which was first reported by Kossard over 20 years ago (13). It is characterized by hair loss on the frontotemporal region of the hair line, followed by a scarred scalp on the affected area (14). It was initially predominantly diagnosed in post-menopausal women (15). However, in the last decade there has been an exponential increase in reported cases (Figure *2*) which include younger women and men, although such cases are rarely reported as compared to those that occur amongst post-menopausal women (6).

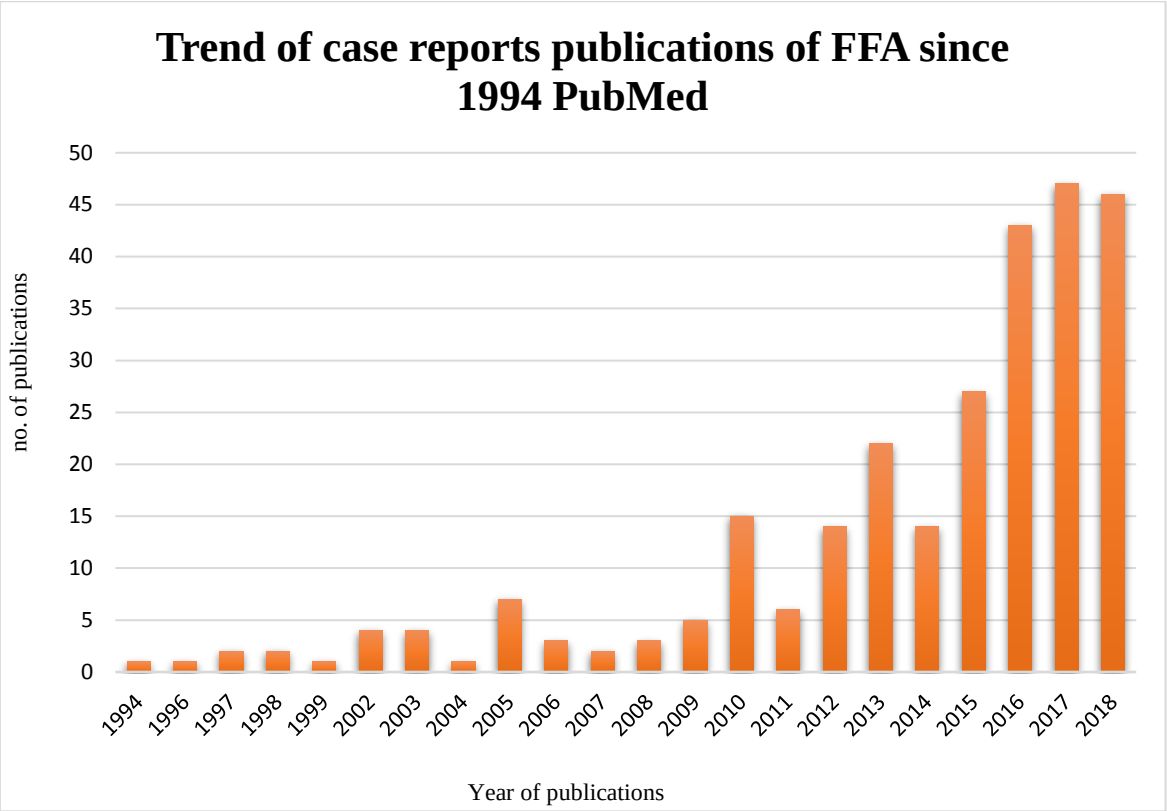

Figure 2 An exponential increase in the number of published FFA case reports over the past decades (PubMed search, July 2018).

The alarming exponential increase of FFA cases over recent years has raised a number of speculations, regarding factors that could be playing a role in its pathobiology (15&16), in particular environmental factors have been mainly suspected (15). Moreover, additional suspicions raised in the study by Aldoori, Dobson (17), further suggests that sunscreens and leave-on facial creams (which increasingly contain UV filters) could be possible environmental factors that are potentially contributing to FFA pathogenesis. In their study, they reported more frequent use of facial sunscreens by FFA subjects as compared to controls.

The exponential increase in reported FFA cases over the past decades seems to also coincide with increased incorporation of nanomaterial-products (especial UV filters) in cosmetic products such as creams, make up powders, hair treatments, lotions and sprays (18&19).

Moreover, these cosmetics products containing nano-materials are termed nanocosmetics (20) and amongst them, the commonly used ingredients are titanium dioxide, silicon dioxide and zinc oxide (18&19). Zinc oxide and titanium dioxide are also considered the most efficient sunscreen/photoprotection active ingredients (21). Titanium dioxide is the UV filter that has been under more scrutiny regarding the sunscreen association with the pathogenesis of FFA. A recent study (22) detected titanium nanoparticle on the hair shaft of a patient affected FFA using SEM/EDS. Thompson, Chen (23) did a pilot study with a bigger sample size (20 patients – 16 FFA and 4 controls) and they detected the presence of titanium particles on the hair shafts of all the 16 subjects + 3 controls. However, due to detection of titanium also in controls, they could not pin titanium as a direct causative factor.

The timeline illustrating the regulation and increase of the commercialized nano-technology incorporated cosmetic products it is shown in (Figure *3*). The time line shows a great increase in these nanocosmetics production in the last decade, which doubled in number (about 100 to 208 products) overlapping with the reported increase in FFA cases.

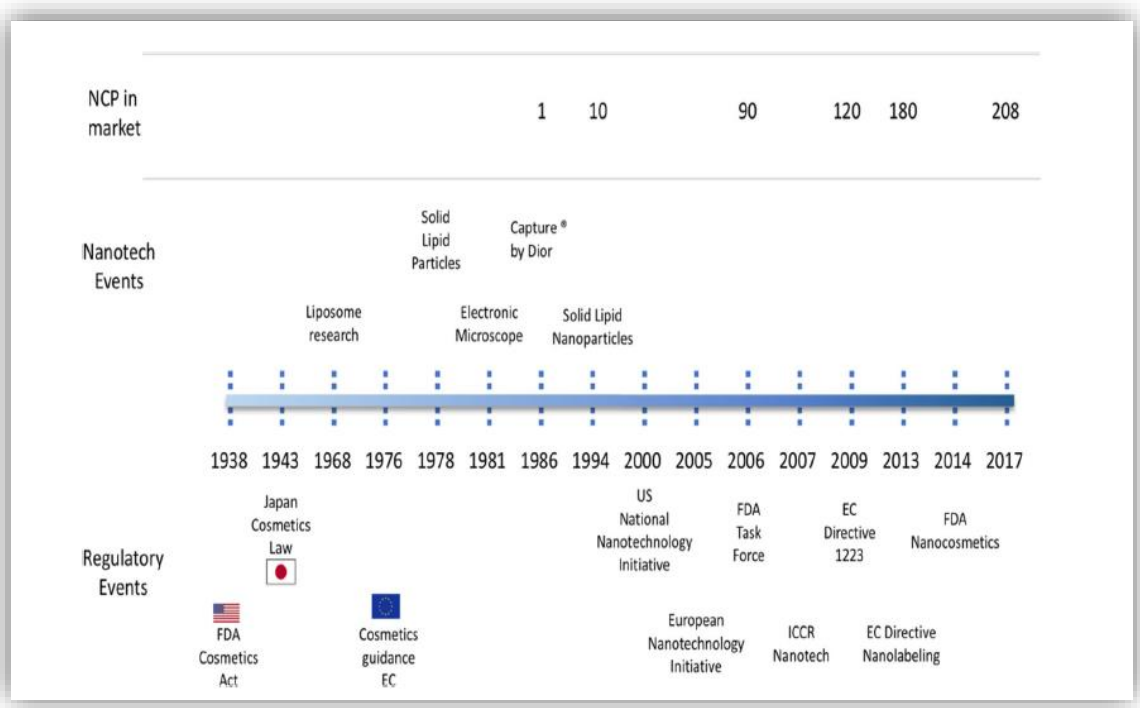

Figure 3 The evolution of the incorporation of nanotechnology in the cosmetic products and the increasing number of products produced over the years (18). NCP (Nanotechnology-enabled cosmetic products)

Sunscreens are topical agents, which contains various ingredients to aid in skin photo-protection against ultraviolet (UV) rays (24&25). The sun's UV radiation is a common cause of skin cancers and photo-aging of the skin (26&27). Topicals for photo-protection are classified into two forms; chemical filters and physical blockers (26&27). Sunscreens have evolved greatly over the decades, with some ingredients being banned due to their toxicity and new ones invented, history of commercial use from the early 90s to date is demonstrated in (Figure *4*).

Year(s)	Development
1928	First commercial use of sunscreen in the United States: emulsion containing benzyl salicylate and benzyl cinnamate[1]
1933	An ointment containing benzylimidazole sulfonic acid becomes the first commercial sunscreen available in Germany[1]
1936	The future founder of L'Oreal, Eugène Schueller, markets the first commercial sunscreen available in France, an oil preparation containing benzyl salicylate[1]
1938	Franz Greiter, the founder of Piz Buin Company, develops an effective sunscreen in Austria, Gletscher crème; he later improves upon and popularizes the concept of SPF (1974)[1]
1943	p-Amino benzoic acid is patented[2]
1950s	Higher incomes and expanding travel options spur emergence of the sunscreen market[3]
1956	Schulze invents the SPF, enabling the evaluation of sunscreen performance[4]
1970s	Introduction of oxybenzone as a broad spectrum UVB/UVA filter; broad introduction of SPF on sunscreen packaging revolutionizes marker, and products are now comparable on a quantitative basis
1980s	Avobenzone, a long-wave UVA filter, is approved by the US FDA (1988; approved in Europe in 1978)
1990s-2000s	Attitude of consumers toward sun exposure changes as the public becomes increasingly aware of the potential harm from solar radiation
2000s-2010s	Role of topical sunscreens expands from mere protection against sunburn to include health prophylaxis

FDA, Food and Drug Administration; *SPF*, Sun Protection Factor; *UVA*, ultraviolet A light; *UVB*, ultraviolet B light.

Figure 4 Evolution history of the sunscreens commercial use (28)

Over recent years, there has been numerous developments of various nanoparticles that have been used in various fields, including sunscreens formulations. Initially, sunscreen formulations were mainly organic chemical UV filters and micron-scale metal oxide UV blockers (29). Metal oxide nanoparticles (NPs) UV filters were then introduced in the last two decades as the most efficient UV filters (21), due to their exceptional properties. Metal oxide nanoparticles (NPs) UV filters, possess both properties of the organic filters and micron-scale inorganic blockers, which are absorbing and scattering light, simultaneously (29).

Hanigan, Truong (29), examined the environmental toxicity of inorganic sunscreen nanoparticles such as ZnO and TiO_2, when exposed to the aquatic system. To investigate the potential toxicity of ZnO and TiO_2, they developed a method to extract these NPs from sunscreens and added parts per million (PPM) concentrations (as typically found in sunscreens) of nano- ZnO and TiO_2 to zebrafish embryos. From these experiments, limited toxicological effect was found on the zebrafish embryos for both ZnO and TiO_2. It was found, that TiO2 was more prone to photoactivation, as compared with ZnO; albeit ZnO was

identified to be more toxic. They concluded that incorporation of NPs into sunscreens may potentially lead to an increase in free radicals in the environment, thereby affect the ecosystem.

There have also been some concerns raised regarding the safety of the use of NPs on human beings, as they have been implicated in several biological systems disruption such as respiratory, cardiovascular, genetic and endocrine systems (21&30&31). An in-vitro study by Khan, Naqvi (31), investigated the genotoxic and cytotoxic effect of zinc oxide and titanium oxide nano-formulations at increasing concentrations, using human lymphocytes and erythrocytes, respectively. It was identified in this study, that hemolytic activities in erythrocytes were concentration dependent for both ZnO and TiO_2. Also, both nanoparticles were found to be cytotoxic to lymphocytes. It was identified that the nanoparticles increased reactive oxygen species (ROS) and decreased the level of glutathione in these cells. Overall, it was identified that zinc oxide was significantly more genotoxic compared to titanium oxide at higher concentration.

De Matteis (30) reviewed the entry mechanism, biodistribution and immunological response of the human body to inorganic nanoparticles. It was pointed out that the physico-chemical properties and size of the NPs ultimately determines their toxicity potential. The review showed that even though the possibility of skin penetration by NPs remains a controversy among researchers, available evidence seems to indicate that penetration of the skin is size-dependent. For example, it was found that NPs of approximately 4nm are able to penetrate intact skin, while NPs of 45nm and higher can only penetrate damaged skin (32). Also, photoactivation, irradiation and pH, have been shown to alter the sizes of NPs, thereby increasing the potential of penetration (33). Smaller, cationic NPs have been found to be more potent in inducing immunological reactions (cytokine release), DNA damage, apoptosis and oxidative stress; as compared with larger NP particles (30).

Moreover, the rise in the sales of sunscreens seems to have coincided with an increase in the prevalence of skin cancers worldwide; and this also has sparked an ongoing controversy regarding their safety in recent years (34). The reasons for increased skin cancer numbers could be the false-sense of security (and increased sun bathing when sunscreens are applied results) but could also be ascertainment bias because more people present to doctors with suspicious skin lesions because of effective public education. The goal of this study is to investigate the association between sunscreen (actives) use and FFA pathogenesis.

FFA is a subtype of PCA which is characterized by an irreversible damage of the hair follicle and replacement by fibrotic tissue. This results in loss of hair follicles, visualized as baldness or scarred skin region (12). Gaspar (35) reported that the hair-loss progression which usually occur on the frontal hairline (Figure 5), may even progress to lateral and posterior directions.

Figure 5 Female recruited participant (61 years) of the study, presenting clinical appearance of FFA via extreme frontal hair loss, accompanied by hyperpigmentation of the face.

Hair loss may also occur in other parts of the body such as eyebrows (36). It is a challenging hair loss disorder first reported in 1994; and to this day, no study has found its exact etiology (37). However, it has been hypothesized that hormonal imbalance associated with

menopause might be one of the triggers that causes FFA in postmenopausal women (13). Further, inflammation around the bulge region, which houses one of the most important cells for the hair cycle, i.e. hair follicle stem cells (HFSCs), results in permanent hair follicle destruction. On the other hand, inflammation affecting the bulb region of the hair follicle typically results in a temporary destruction of the hair follicle and thereby results in potentially reversible alopecia such as in alopecia areata (Ge *et al*., 2017; Harries, Meyer, & Paus, 2009) (Figure *6*).

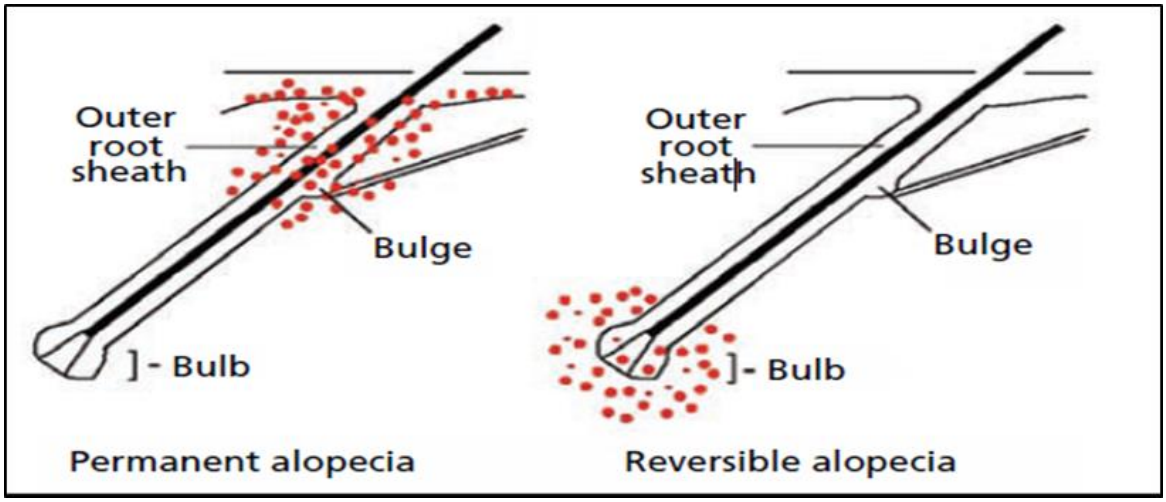

Figure 6 Illustration of hair follicle inflammation. Reversible alopecia (right) is characterized by damage to the hair bulb from inflammation. Cicatricial alopecia (left) is characterized by inflammation that causes irreversible damage to the hair bulge of the outer root sheath the location of stem cells (12).

1.1.1 EPIDEMIOLOGY

There has been an exponential increase in the number of frontal fibrosing alopecia (FFA) cases over the last decade since the year 1994 when it was first described. This raises suspicion of the possible role of an environmental causative factor for its etiopathogenesis. The multicenter study by Vano-Galvan, Molina-Ruiz (38) reported the highest number of FFA (355) cases (including premenopausal women and men) from 12 Spanish centers in Spain. In South Africa (SA), there have been a few case reports on FFA patients, including

both male and female (39-41). However, no epidemiologic data on sunscreen use (describing types, formulation and frequency of use) has been published regarding the FFA cases in SA.

1.1.2 CAUSATIVE AGENTS

Frontal Fibrosing Alopecia could be considered a multifactorial disease, due to the number of suspected etiopathogenetic factors such hormonal, autoimmune defense mechanisms, environmental and genetic factors (42). However, little or no laboratory or clinical research has been done to confirm these hypotheses.

1.1.2.1 Immune system defence mechanisms

Autoimmune response has been one of the highlighted factors believed to be behind the cause of FFA and other PCA. This is responsible for one of its histopathological characteristics which is described as a dense inflammatory infiltrate around the hair follicle (15&43-45), Figure *7* illustrates a histological image of a scalp tissue affected by FFA. Apart from the commonly reported lichenoid inflammatory infiltration and fibrosis around the hair follicle, Miteva, Castillo (45), reported a new potential histological characteristic of FFA, which is the infiltration of fat cells in the dermis and arrector pili muscle. The authors did not elucidate how this observation is related to the destruction of the hair follicle. However, being a consistent histological feature of FFA cases (as compared to the controls they used) indicates a need for further investigation of the role of fat infiltration in the pathogenesis of FFA.

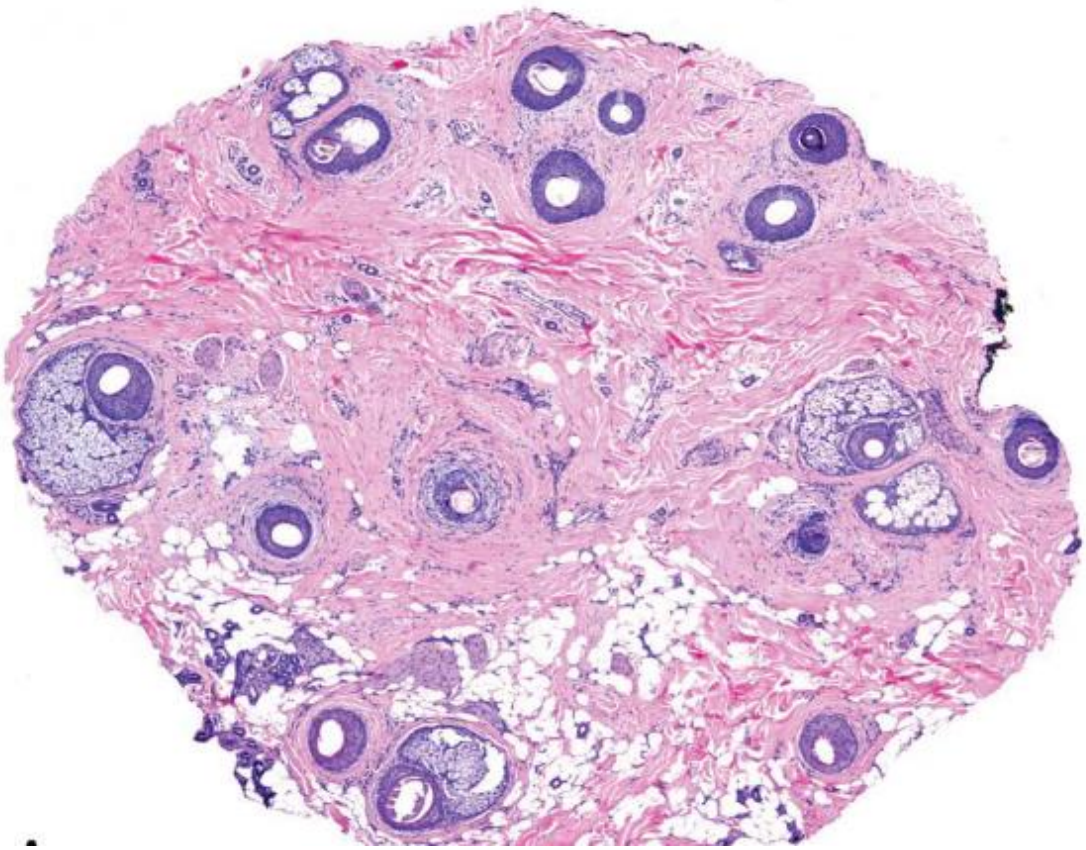

Figure 7 Histological cross sectional image of FFA scalp biopsy, showing inflammatory infiltrate (purple granules) around the hair follicle and adipose tissues (45).

The most crucial part needed for hair regeneration is believed to be the hair follicle bulge; and PCA results if it is compromised (46). The hair follicle bulge is known as an organ which houses the hair follicle's most significant cells termed hair follicle stems cells (HFSCs), which are responsible for the regeneration of the hair shaft and other important components of the hair follicle (46-48). Therefore, any damage to these cells could either interfere with the hair regeneration cycle or completely bring it to a stop (49). Ma, Imadojemu (36), demonstrated that these autoimmune inflammatory features of FFA are possibly related to the fact that Langerhans cells (LCs) and CD8+ T cells were the most abundant cells in inflammatory infiltrates from the infundibulo-isthmic region. Thereby, hypothesizing that the LCs may be the stimulus for the response of CD8+ T cells, resulting

in the initiation of inflammatory reactions. However, this hypothesis still does not explain how or what initiates the inflammatory reaction.

1.1.2.2 Hormonal factors

Another suspected underlying factor for the pathogenesis of FFA is hormones. They were the first underlying factors to be implicated when FFA was first described by Kossard two decades ago, and this was due to its predominance in post-menopausal women (35). The hormone Dehydroepiandrosterone (DHEA) is one of the implicated hormones (50); it has immunomodulatory effect on a gene termed peroxisome proliferator-activated receptor (*PPAR).* The *PPAR* is thought to control fibrogenic activity of transforming growth factor-beta 1 (*TGFβ1*) (35). Gaspar (35) also stated that there are reports, claiming a decrease of DHEA in some fibrotic processes, but no evidence connects it directly to the fibrosis of a permanently damaged hair follicle. Ranasinghe, Piliang (50) reported hormonal dysfunction in patients affected by FFA, particularly implicating androgen hormones, which are also a main causative factor in male pattern baldness. A number of case reports demonstrated the effectiveness of antiandrogen therapy in FFA cases (51), and also gives basis for the implication of the androgen hormones in the pathogenesis of FFA and lichen planopilaris (LLP) (50).

1.1.2.3 Environmental factors (cosmetic products)

Frontal fibrosing alopecia case reports have shown an exponential increase over the past decade, which raised a suspicion of possible involvement of an environmental factor in its etiopathogenesis (52). Cosmetic products have been one of the suspected environmental causative agents, which could lead to the development or progression of FFA; more especially sunscreens and facial creams containing sun protection factors (SPF) (16&17). However, no experimental work has been done to confirm or refute this suspicion; only

questionnaire-based studies have been done. It has been suggested that cosmetic products' active sun protective ingredients may alter the integrity of important biological components such as proteins and DNA; especially if they are in nano particle size (53-55). Moreover, their photochemical instability is reported to lead to formation of reactive oxygen species (ROS), inducing disruption of the individual physiological metabolic response (53&55&56). Common sunscreen active ingredients include titanium oxide, zinc oxide, ethylhexyl dimethyl paba, octylmethoxy cinnamate, benzophenone-3 and homosalate (57&58). However, with no strong scientific proof of penetration of these ingredients through human skin and disruption of the normal functioning of biological systems such as endocrine activities (56), the controversy of sunscreen use and the negative impact they may have on human's health still continues. The debate over the use and safety of these sun protection agents (particularly those containing nano-preparations) has gained momentum over the past years; with an exponential rise in the number of published observational studies (Figure *8*).

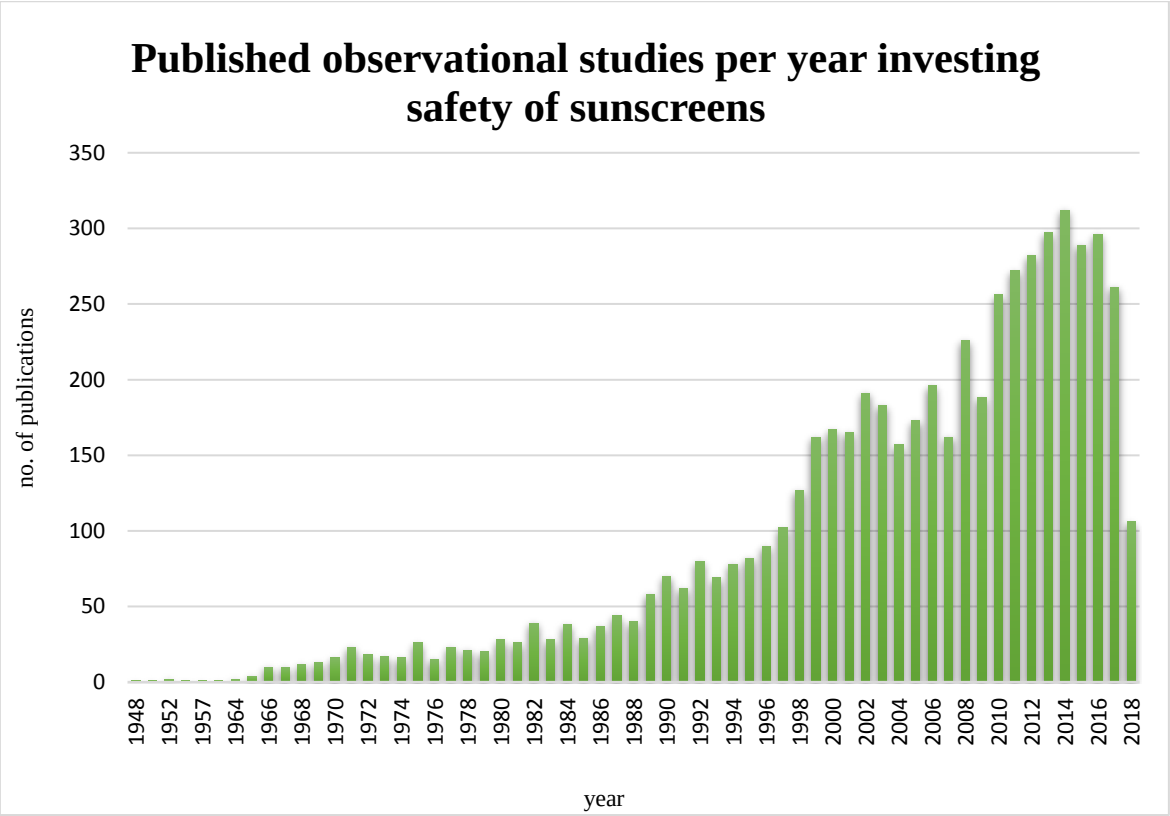

Figure 8 shows an exponential rise in the number of observational studies regarding safety concerns and rise of their usage (PubMed search, July 2018).

Photo protection creams have been the topic of research interest over the years (59), with special scrutiny with regard to their safety (59). This ongoing debate led to many sunscreen actives being banned and introduction of strict regulations regarding their manufacturing and usage, in regions such as Europe, United State, Japan and Australia (60&61). The currently approved common sunscreen actives by the Food and Drug Administration (FDA) are listed below **(**Figure *9***)**. These actives are usually divided into two categories, chemical and physical.

Table II. FDA-approved active sunscreen ingredients

FDA-approved†active sunscreen ingredient	Maximum FDA-approved concentration (%)	Peak absorption wavelength (nm)	Range of protection (nm)	Protection provided (UVB/UVA)
Inorganic				
Titanium dioxide	25.0	Varies	290-350	UVB, UVA2
Zinc oxide	25.0	Varies	290-400	UVB, UVA1
Organic UVB				
PABA	15.0	283	260-313	
Padimate O	8.0	311	290-315	
Octinoxate (octyl methoxycinnamates)	7.5	311	280-310	
Cinoxate	3.0	290	270-328	
Octisalate (octyl salicylate)	5.0	307	260-310	UVB
Homosalate	15.0	306	290-315	
Trolamine salicylate	12.0	260-355	269-320	
Octylocrylene	10.0	303	287-323	
Ensulizole (phenylbenzimidazole sulfonic acid)	4.0	310	290-340	
Organic UVA				
Oxybenzone	6.0	290, 325	270-350	UVB, UVA2
Sulisobenzone	10.0	366	250-380	UVB, UVA2
Dioxybenzone	3.0	352	206-380	UVB, UVA2
Meradimate (menthyl anthranilate)	5.0	336	200-380	UVA2
Avobenzone	3.0	360	310-400	UVA1, UVA2
Ecamsule (terephthalydene dicamphor sulfonic acid [Mexoryl SX])	10.0	345	295-390	UVA1, UVA2

†FDA approved as of Dec. 7, 2009.

Figure 9 Common sunscreen actives approved by FDA (61).

1.1.2.4 Genetic factors

Genetics has also been implicated in the etiopathogenesis of FFA, due to the increasing identification of familial FFA cases since the condition was first described (62). Muireann Roche and colleagues (63) were the first to report FFA familial case. In 2019, Porrino-Bustamante, Lopez-Nevot (64) reported a large case series of 20 individuals from 9 families presenting with familial FFA cases. These evidences strengthen the suspicion of the possible role of genetic factors in the etiology of FFA. Human leukocyte antigen (HLA) complexes have been one of the great topics of interest regarding the genetic aspect of FFA etiopathogenesis (65-67). HLA genes codes for proteins that are responsible for presenting antigen to immune defense complexes such T-lymphocytes (68). These T-lymphocytes are activated by both the HLA I and II class antigenic peptides in an adaptive immunity response (69). These two histocompatibility complex classes are commonly associated with autoimmune resistance and susceptibility to infections, diseases and autoimmune initiated

illnesses (70). Class I is responsible for the self-immunity, whereas class II drives the non-self-immunity (71).

A recent study reported a gene (CYP21A2 gene p.V281L) mutation that could be potentially associated with FFA patients' susceptibility to the development of the hair loss disorder, which is linked to the human leukocyte antigen (HLA) class I haplotypes (67). This was followed by a genome-wide association study (GWAS) study by Tziotzios, Petridis (72) which also implicated the four genomic loci: 2p22.2, 6p21.1, 8q24.22 and 15q2.1 which are driven by HLA-B*07:02 as the genetic predisposition marker for FFA. These studies shed a great light on the genetic aspect of FFA and could be used as a guide into researching further and elucidating the genetic factors that play a role in the pathogenesis of FFA.

1.1.3 TREATMENT AND MANAGEMENT

Several studies have reported treatment of cases of the FFA, however, up to date no specific curative treatment has been discovered (12&73). Most studies report treatments that may slows down the progression of the scarring hair-loss, by reducing disease activity (73). Medications that have been used include doxycycline, dutasteride, pimecrolimus, hydroxychloroquine and finasteride (74-76) (Figure *10*). There is variable response to these treatment (12&74), which is complicated by the paucity of randomized controlled trial or meta-analysis evidence. Moreover, treatment related side effects such as hyperpigmentation of the skin, breast tenderness and sexual dysfunction have been reported (74), with no evidence on which exact agents within this medication causes these side effects (73&74).

Agent	Studies	Dosing	Frequency	No. of Patients	Response %	Overall Response %
Prednisolone	Rallis et al[31]	16 mg	Daily	1	100	100
ITA	Banka et al[9]	2.5 mg/mL × 0.5-3 mL	Every 6-8 weeks	62	97	56
	Donovan et al[44]	0.125 mL/eyebrow	NA	11	64	
	Kossard et al[2]	NA	NA	1	0	
	MacDonald et al[12]	10 mg/mL	NA	8	0	
	Moreno-Ramirez and Camacho Martinez[15]	20 mg/mL (1 mg/2 cm^2)	Every 3 months	15	93	
	Vañó-Galván et al[3]	NA	Every 3-6 months	130	34	
	Tan and Messenger[13]	10 mg/mL	NA	12	67	
Dutasteride	Georgala et al[51]	0.5 mg	Daily	13	62	56
	Ladizinski et al[4]	0.5 mg	Weekly	10	70	
	Vañó-Galván et al[3]	0.5 mg	Weekly	18	44	
Finasteride	Ladizinski et al[4]	1-2.5 mg	Daily	3	33	47
	Rallis et al[31]	2.5 mg	Daily	5	60	
	Tosti et al[14]	2.5 mg	Daily	8	50	
	Vañó-Galván et al[3]	2.5-5 mg	Daily	102	47	
Prednisone	Kossard et al[2]	25-50 mg	Daily	4	50	40
	MacDonald et al[12]	NA	NA	1	0	
Topical minoxidil	Kossard et al[2]	2% solution	NA	2	0	39
	MacDonald et al[12]	NA	NA	3	0	
	Rallis et al[31]	2% solution	NA	5	60	
	Tosti et al[14]	2%	Twice daily	8	50	
Chloroquine	Kossard et al[2]	150 mg	Daily	3	33	33
Topical CS	Kossard et al[2]	NA	NA	9	0	25
	Rallis et al[31]	Clobetasol 0.05% solution	Daily	6	50	
	Tan and Messenger[13]	NA	NA	1	100	
Doxycycline	Samrao et al[10]	NA	NA	4	25	25
MMF	Samrao et al[10]	NA	NA	5	20	20
HCQ	MacDonald et al[12]	NA	NA	9	0	18
	Ladizinski et al[4]	400 mg	Daily	4	50	
	Samrao et al[10]	NA	NA	16	25	
	Tan and Messenger[13]	NA	NA	2	50	
	Vañó-Galván et al[3]	200-400 mg	Daily	54	15	
Topical CI	MacDonald et al[12]	NA	NA	22	0	0
Triamcinolone	Tosti et al[14]	40 mg IM	Every 3 weeks	3	0	0

Abbreviations: CI, calcineurin inhibitor; CS, corticosteroid; HCQ, hydroxychloroquine; IM, intramuscular; ITA, intralesional triamcinolone acetate; MMF, mycophenolate mofetil; NA, not applicable.

Figure 10 Shows the tried treatment for and their level of efficacy (51).

1.2 PROBLEM STATEMENT

The recent increase in reports and poorly understood etiology makes FFA a disease of clinical and psychosocial significance (77) across the world. Initially FFA was thought to be a disease of postmenopausal women, who may have morbidities associated with hormonal changes and age. However, recent evidence suggests the increasing number of affected men and premenopausal women (12&16&35&42). This makes FFA, a growing public health problem. With poorly understood etiology and ineffective treatment, FFA is taking an increasing share of the health budget.

1.3 SIGNIFICANCE OF THE STUDY

The number of FFA cases have increased worldwide since the handful reported by Kossard in Australia in 1994. With the use of cosmetic creams suspected as contributors to the development of FFA, this study aimed to conduct a laboratory evaluation of possible associations between sunscreen actives and FFA. The identification of an association between FFA and an environmental exposure, could assist in preventing and/or reducing the risk of developing FFA which would reduce the burden on the health budget.

1.4 AIM

The aim of the study it is to investigate whether there is an association between frontal fibrosing alopecia (FFA) and sunscreen actives.

1.5 HYPOTHESIS

- H_0: there is no association between sunscreen actives and the pathogenesis of frontal fibrosing alopecia (FFA).
- H_A: There is an association between sunscreen actives and the pathogenesis of FFA.

1.6 OBJECTIVES

- Detect and compare the presence of sunscreen actives in the frontal fibrosing alopecia (FFA), lichen planopilaris (LPP) and traction alopecia (TA) formalin-fixed paraffin embedded (FFPE) sections using:
    i. Scanning electron microscope (SEM)/ Energy-dispersive X-ray spectroscopy (EDS).
    ii. Fourier-transform infrared spectroscopy (FTIR) comparison using multivariate analysis Orthogonal Partial Least Squares Discriminant Analysis (OPLS-DA). and SIMCA (Software Independent Modelling of Class Analogy).

- Determine the cytotoxicity effect of 5 sunscreen actives (titanium dioxide, zinc oxide, octyl methoxycinnamate, benzophenone-4 and 2-ethylhexyl dimethyl PABA) on monolayer of immortalised human keratinocyte (HaCaTs), FFA tissue-derived fibroblasts and normal scalp tissue-derived fibroblasts.

    i. Cell counting kit 8 cell viability kit (CCK-8)

- Investigate energy phenotype switch of HaCaTs, FFA tissue-derived fibroblasts and normal scalp tissue-derived fibroblasts, after 24 hours treatment with sunscreen actives using the Seahorse extracellular flux bioanalyser.

CHAPTER 2

2. METHODOLOGY

2.1 STUDY PARTICIPANTS AND SAMPLES

Four participants were recruited as tissue donors for the study: females between the age of 55 and 61 years old, with an age average of 59, who were diagnosed with FFA. A total of 25 (9 FFA, 11 LPP and 5 TA) biopsies were obtained from archives of the local National Health Laboratory Service (NHLS) repository, into which patient biopsy samples from Groote Schuur Hospital are routinely evaluated for diagnosis and stored.

Table 1 Demographic data of the FFA, LPP and TA participants, whom the tissue was biopsied from.

Alopecia Type	Coding	Gender	Age	Mean Age
Frontal Fibrosing Alopecia	FFA 01	M	55	63
Frontal Fibrosing Alopecia	FFA 02	F	66	
Frontal Fibrosing Alopecia	FFA 03	F	69	
Frontal Fibrosing Alopecia	FFA 04	F	72	
Frontal Fibrosing Alopecia	FFA 05	F	64	
Frontal Fibrosing Alopecia	FFA 06	F	61	
Frontal Fibrosing Alopecia	FFA 07	F	54	
Frontal Fibrosing Alopecia	FFA 08	F	56	
Frontal Fibrosing Alopecia	FFA 09	F	74	
Lichen Planopilaris	LPP 01	M	65	52
Lichen Planopilaris	LPP 02	F	55	
Lichen Planopilaris	LPP 03	F	59	
Lichen Planopilaris	LPP 04	F	72	
Lichen Planopilaris	LPP 05	F	41	
Lichen Planopilaris	LPP 06	F	61	
Lichen Planopilaris	LPP 07	M	26	
Lichen Planopilaris	LPP 08	M	53	
Lichen Planopilaris	LPP 09	M	42	
Lichen Planopilaris	LPP 10	M	51	
Lichen Planopilaris	LPP 11	F	49	
Traction Alopecia	TA 01	F	30	40
Traction Alopecia	TA 02	F	29	
Traction Alopecia	TA 03	F	53	
Traction Alopecia	TA 04	F	48	
Traction Alopecia	TA 05	F	41	

2.2 ETHICAL CONSIDERATIONS

The study was approved by the University of Cape Town Human Research Ethics Committee (HREC: #759/2017). Participation was voluntary, and each participant signed a written consent form upon agreement to take part in the study. Permission was also granted (HREC: #153/2017) to use pathology archives from the National Health Laboratory Services (NHLS) at Groote Schuur Hospital, samples from patients with FFA, LPP and TA. The reason for choosing to compare with these two conditions was because LPP has a similar histology and TA a similar anatomical location with FFA.

2.3 RESEARCH SITE

All the participants were recruited from the Groote Schuur Hospital (Hair Clinic), Cape Town, South Africa.

2.4 MICROSCOPIC ANALYSIS OF SUNSCREEN ACTIVES TRACES ON FORMALIN-FIXED PARAFFIN-EMBEDDED (FFPE) SECTIONS

2.4.1 Formalin-fixed paraffin-embedded sections

FFPE sections (5 µm) of FFA, TA and LPP biopsies were used for microscopy analysis. These archival tissues are used for routine diagnosis and then stored by the NHLS. The sections were mounted on standard hematoxylin and eosin (H&E) staining microscopic glass slide before observation under SEM and FTIR. The glass slides were dewaxed following a standard protocol (78). Firstly, the slides were heated at 60° C for 15-30 minutes; thereafter, the slides were incubated in three xylene baths for 3 minutes each, followed by incubation sequentially in 3 baths containing ethanol (100%, 96% and 70% for a minute each). Thereafter, the slides were rinsed in water and allowed to air dry before any analysis was done on them. Using both SEM and FTIR increased the potentially be a complementary

suite of microscopic/spectroscopic elemental and chemical group analysis as performed here.

2.4.2 Scanning electron microscope (SEM) & Energy-dispersive X-ray spectroscopy (EDS)

SEM it is a form of a microscopy imaging technique which uses a beam of highly energetic electrons as its source of illumination, to form a focused image of a specimen of interest (79). It performs this function by scanning a specimen of interest with a beam of electrons, resulting in an image of high resolution of down to 0.02 nm, for 100 kV electrons (79). The electron beams interact with the atoms contained in the specimen, to give out any information concerning the specimen. Information such as the chemical composition of the specimen, its morphology and topography (80&81).

EDS it is a technique well-known for the elemental identification of materials through the energy excitation of X-ray lines of the analyte of interest (82&83). EDS generates an X-ray spectrum of the analyte, from its scanned image area by SEM. This x-ray spectrum shows elements at their different shell energy levels (84).

The FFPE glass slide of each sample was mounted by a carbon tape onto the SEM sample holder and inserted in the instrument to produce an image of the tissue. After the image was obtained, the SEM's Energy-dispersive X-ray spectroscopy (EDS) source was used to obtain chemical characterization of the tissue by analysing elements contained on the tissue. Varying EDS energy levels were used to detect elements on each sample, since each element has a specific energy level to excite it from a resting state. Therefore, to ensure that all the elements which were present on each sample were detected, the following energy levels were used: 5kV, 10kV, 15kV and 20kV (85).

2.4.3 Fourier-Transform infrared (FTIR) spectroscopy

FTIR is a technique used to collect high infrared spectral resolution data of emission or absorption for a liquid, solid or gas, over a wide range; using a mathematical process (Fourier Transform) to generate actual spectral data. FTIR can be used to carry out functions such as identification of chemical groups or contamination analysis on biological tissues (86). It does so by giving a molecular fingerprint of the sample through triggering vibrations on its molecular bonds by irradiation with infrared light (87). This molecular vibrations provide information such as the presence of functional groups in the sample in a form of a spectrum with varying peaks, thus giving an insight about components contained in the sample (87). The technique has three methods; transmission, reflectance and Attenuated total reflection (ATR), which are used according to the type of a sample analysed. In this study, one of the aforementioned platforms was used i.e ATR, (88-90). FFPE sections were used for the FTIR analysis, following the dewaxing procedure as previously prescribed.

2.4.4 MULTIVARIATE STATISTICAL ANALYSIS OF THE ATR-FTIR SPECTRA DATASET

Multivariate analysis is a statistical technique used to simultaneously investigate the relationship between multiple outcome variables of interest in a single context (MKS Umetrics, version 13). Software independent modelling of class analogy (SIMCA) it one of the well-known software which enables such analysis. In this study, a SIMCA discriminant classification model termed Orthogonal Partial Least Squares-Discriminant Analysis (OPLS-DA) was used to evaluate a systematic variation within the FTIR spectra of the FFPE scalp sections of FFA, LPP and TA. The OPLS-DA model is a technique used to detect variation on a large set of data obtained from model that puts FTIR data into two categories (predictive and orthogonal variation) (91). Prior to that, another multivariate model called principal component analysis (PCA) was performed on the dataset. The PCA model enables

an overview of the dataset of interest, showing an overall systemic patterns of variation on the entire data set of variables (92). The PCA results obtained (**Appendix 2**) did not show a distinctive separation between the dataset of all the three hair loss conditions combined, hence, the OPLS-DA model was found to be a better multivariate model to evaluate systemic variations within the dataset.

2.5 In vitro cytotoxicity models

2.5.1 Cells and culture conditions

In this study, two cell types were used, namely patient-derived fibroblasts (PDF) and immortalised human keratinocyte (HaCaTs) cell line. PDF were isolated from patients affected with FFA at Groote Schuur Hospital (Cape Town, South Africa), following informed consent from patients, and ethical approval (HREC # 759/2017) from the Human Research Ethics Committee of the Faculty of Health Sciences, University of Cape Town.

Briefly, skin tissue (4 mm punch biopsy) was transported in 10ml Dulbecco's Modified Eagle's Medium (Highveld Biological, South Africa) supplemented with 100U/ml Penicillin/ 100µg/ml Streptomycin (Sigma-Aldrich, South Africa) upon collection from the hospital. Excess adipose tissue was aseptically removed from the tissue. The epidermal part was removed with a surgical blade (KIMIX, South Africa), while dermal part, was cut into small pieces and placed in a NEST 6 well tissue culture plates (Thermofisher, South Africa). Deckglaser microscope glass cover slips (Fisher scientific, South Africa) were used to hold the tissue in place. This tissue was then incubated at 37^{o}C until fibroblast explants formed confluent monolayers, with culture media changed every third day. Both cell types were cultured on separate 10 cm tissue culture dishes (Thermofisher, SA), in Dulbecco's Modified Eagle's medium (DMEM) enriched with 10% fetal bovine serum **(**FBS) and 1% penicillin and streptomycin (P/S), namely complete DMEM. Thereafter, they were incubated in an

incubator (SHEL LAB, United States of America), under the following conditions; temperature of 37 ^{0}C, 95% relative humidity and 5% carbon dioxide. The cells were allowed to grow to confluency, with the culture medium being changed every third day. Resultant fibroblasts were cultured and propagated in complete DMEM, stored until further use. Cells were used until passage #6.

2.5.2 Sunscreen actives preparation

Five sunscreen active ingredients were used, both physical and chemical. Titanium dioxide (Savannah Fine Chemicals, SA) and zinc oxide (BASF, South Africa) nano powders were dispersed in 10% propylene glycol solution, respectively. Octyl methoxycinnamate (BASF, SA) and ethylhexyl dimethyl PABA (ASHLAND, USA) were resuspended in 0.05% sodium lauryl sulfate (SLS) solution, (Sigma-Aldrich, SA). Benzophenone-4 (BASF, SA) was dissolved in distilled water. The different solvents were used to resuspend the sunscreen active ingredients, and this was due to their different solubility properties. Titanium dioxide and zinc oxide were dispersed in water-oil emulsion (prop-glycol), as it is reported as a good vehicle to prevent the aggregation of the nanoparticles (as they are poorly soluble in water). The water-oil emulsion improves dispersion of the particles and prevents them from aggregating (93&94). The oil based Octlyl methoxycinnamate and ethylhexyl dimethyl PABA solutions were resuspended in SLS which is anionic surfactant commonly used for emulsifying oils (95). This was done to stabilize the dispersion of the Octlyl methoxycinnamate and ethylhexyl dimethyl PABA oil solutions.

Moreover, before these solvents were used, their cytotoxicity was tested by treating the cells with them for 24 hrs and they were found to have a negligible effect on the cells. They were prepared in concentrations outlined in *Table 2*. The calculations for the preparations of these concentrations are clearly outlined in **Appendix 3**.

Table 2 Prepared concentrations of the sunscreen actives

	Active	**Concentration (%)**				
Physical	Titanium dioxide	5	4	3	2	1
	Zinc oxide	5	4	3	2	1
Chemical	Octyl methoxycinnamate	7.5	5	3.5	2	1
	Benzophenone-4	7.5	5	3.5	2	1
	2-ethylhexyl dimethyl PABA	15	10	5	2.5	1

Table 3 The table of the function, physical and chemical properties of the sunscreen active ingredients used on the study (PubChem).

Active	Range	Max %	Function	Reactivity
Titanium Dioxide Chemical formula: TiO_2 Molar mass: 79.866 g/mol Density: 4320 kg m^{-3} Melting point: 1,843 °C Boiling point: 2,972 °C	UVB, UVA2	25%	Reflects and blocks UVA and UVB rays, however, it doesn't protect against the whole range of UVA rays.	Photostable; Less likely to cause irritation but may cause breakouts for some people; Responsible for a sunscreen's "white cast"; FDA approved.
Zinc Oxide Molecular Formula: ZnO Formula weight: 81.389 g/mol Melting point: 2248°C; 1975°C Boiling point: sublimes at 1800 °C Density: 5600 kg m^{-3}	UVB, UVA1, UVA2	25%	Absorbs and blocks UVA and UVB rays and therefore is considered "broad-spectrum"	Photostable; Less likely to cause irritation; Responsible for a sunscreen's "white cast"; FDA approved.
Octinoxate Chemical formula: $C_{18}H_{26}O_3$ Molar mass: 290.40 g·mol−1 Density: 1.01 g/cm3 Melting point: −25 °C Boiling point: 98 to 200 °C	UVB	7.5%	Absorbs UVB rays	Water-insoluble; Degrades overtime when exposed to sunlight, therefore not the most photostable; Can be stabilized by other UV filters such as Tinosorb M; Absorbed by skin so there are some safety concerns; FDA approved
Padimate O Chemical formula: $C_{17}H_{27}NO_2$ Molar mass: 277.41 g·mol^{-1} Density: 0.99 g/cm3 Melting point: <25 °C Boiling point: 362 °C	UVB	8%	Absorbs UVB rays	Water-insoluble PABA derivative; Controversial active because after absorbing UVB rays, the active may produce indirect DNA damage. This UV filter is less common in newer sunscreen formulations because it may be an irritant for those with sensitive skin.
Benzophenone-4 Chemical formula: $C_{14}H_{12}O_6S$ Molar mass: 308.304 g/mol Density: 1.262 g/cm^3 Melting point: 145 °C	UVA, UVB	7.5 %	Absorbs UVA and UVB rays	Water-soluble UVA & UVB filter. Used primarily as UVA filter. Does not penetrate the skin to a large degree, but enhances the ability of other ingredients to penetrate. Helps to stabilize UV sensitive formulations such as hair dyes, hair sprays and colour enhanced formulations.

2.5.3 Cytotoxicity Assays

Cytotoxic assays are used to analyse the ability of certain chemicals or cellular mediators to induce cell deaths when they encounter. In this study, we set out to determine the in-vitro effect of sunscreen actives on monolayer cell models. PDF and HaCaTs were utilised in this study. Assay called Cell Counting Kit-8 (CCK-8) (Sigma-Aldrich, SA), was performed for cytotoxic study.

2.5.4 Cell Counting Kit-8 (CCK-8) assay

CCK8 is a sensitive colorimetric assay for determining the viability of cells and cytotoxicity, due to its nonradioactive property. It uses the highly water-soluble tetrazolium salt (WST-8), by reducing it by dehydrogenases in cells into a yellow formazan product, using electron carrier termed 1-Methoxy PMS. The colour intensity of the resultant formazan dye is directly proportional to the number of viable cells. The detection sensitivity of CCK-8 is higher than the other tetrazolium salts such as MTT, XTT, MTS or SRB (96&97) some of those advantageous properties are listen in Table *4*. The reasons for choosing CCK8 and not the other cytotoxic assays are listed below:

- MTT- requires solubilization of the formazan crystals, therefore, incomplete solubilization of formazan crystals can give false negative results for the viability cells (98&99) .
- XTT- assays is not reliable to use on cells with low metabolic activity, therefore changes in the reductive capacity of the cells due to environmental factors such as pH and cell cycle variation may alter final results (98&99).
- SRB- its optimal results depend on the homogeneity of the cell suspension, therefore, presence of aggregated cells may results in unreliable results (98).

- LDH- cell culture medium containing fetal calf serum may alter the assays mechanism, as the serum has inherent activity which could give false positive results (98).

Moreover, CCK8 it is a ready-made solution requiring no premixing with other components, requires no formazan solubilisation step as it is water-soluble, thereby eliminating interferences. Therefore, we used this assay to evaluate the possible cytotoxic effects of sunscreen actives on cells.

Table 4 Advantageous properties of CCK 8 compared to other cell assays (100)

	MTT	MTS	CCK-8	SRB
Solubility	Indissolvable	Water soluble	Water soluble	Indissolvable
Detection Wavelength	490nm	450nm	450nm	510nm
Character	Solid	Liquid	Liquid	Liquid
Usage	Prepare the solutions	Use it right after it was ready	No need to prepare	Prepared beforehand
Need to redissolve or not	Yes, by DMSO	No	No	Yes, by Tris-base solution
Convenience	++	+++	+++	+
Detection speed	+	++	+++	+
Repeatability	+	++	+++	++
Stability	+	+	++	+++

2.5.5.1. CCK8 assay procedure

Cells were washed twice with 1 ml of 1X PBS following the removal of the culture medium. This was followed by the trypsinisation with 1 ml of 0.05% trypsin + EDTA (TE) solution, (Gibco, USA). After adding TE, the dish was placed back into the incubator for about 5 minutes, to allow for cells' detachment from the dish. Thereafter, the TE was inactivated by 2 ml complete DMEM. The cell suspension was then transferred into a 15 ml tube and centrifuged at 1 800 rpm for 3 minutes. After the centrifugation, the supernatant was discarded, and a cell pellet was suspended in complete DMEM. To count cells, 10 µl cell suspension was added to 10 µl trypan blue stain solution (Invitrogen, US). Thereafter, the 10 µl cells in trypan blue solution was placed on a 0.0025 mm2 Neubauer counting chamber

(Marienfield, Germany). About 5000 cells were platted per well in a 96-well plate (Sigma, SA) and allowed to adhere for 24hours before treatment with the actives. After 24 hours incubation, the cells were treated with 10 µl of each active concentration (*Table 2*) in triplicates and was incubated for another 24 hours before adding CCK8 reagent. Following the 24 hrs treatment, medium containing sunscreen actives was removed. Thereafter, the cells were first washed twice with 100 µl 1X PBS, before adding the 10 µl CCK8 reagent to avoid auto photoactivity of the actives (especially TiO2 and ZnO) when reading on a microplate reader. After the washing of cells, 10 µl of the CCK8 solution was added to (90 µl DMEM^{++} cells) solution in each well and the plate was placed and left to incubate for another 4 hrs before reading on a Varioscan microplate reader (Thermofisher, SA). And the assay's action of mechanism it is illustrated in (Figure *11*)

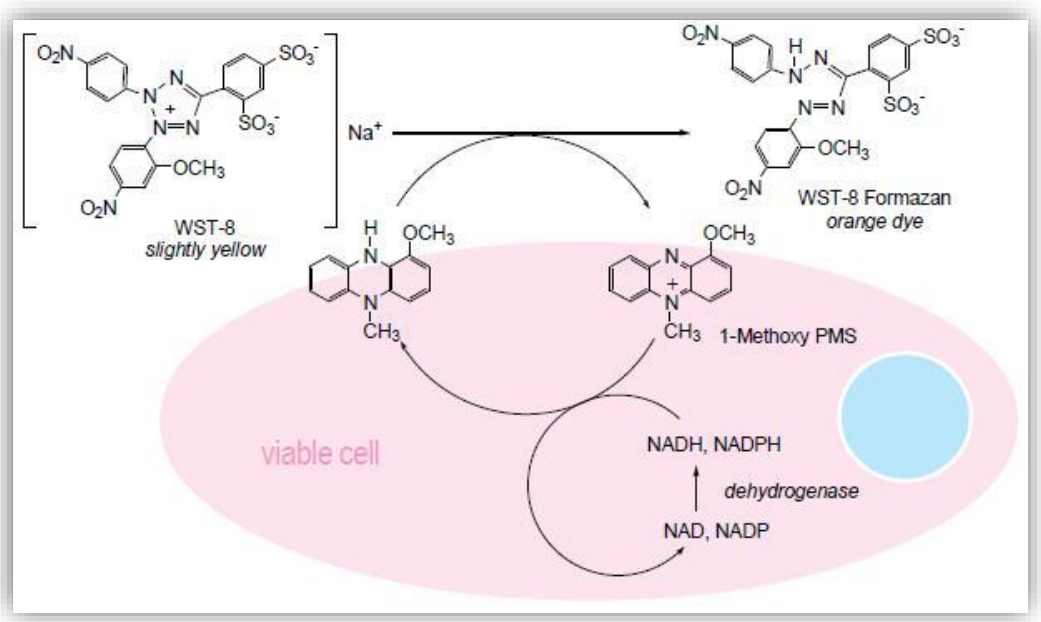

Figure 11 CCK-8 mechanism diagram (Dojindo Molecular Technologies)

Since CCK 8 is a colorimetric assay, the viability of the cells is shown by a colour change of the reagent from its original solution colour to a formazan dye colour. CCK 8 coverts from its pink solution to an orange formazan dye. The more intense the formazan colour is,

the more viable the cells are. The CCK8 assay showed more reliable results compared to the MTT assay (from preliminary studies), confirming what was mentioned by Terry, Richard (101), that it is the most reliable cytotoxicity assay as compared to the other already established cytotoxic assays. Data was analysed using Pearson correlation test and 1-way ANOVA with Kruskal-Wallis post-test with GraphPad Prism 5.

2.5.7 Extracellular flux energy phenotype assay (Agilent Seahorse X96)

Seahorse XF^{e}96 cell energy phenotype test is used to evaluate the metabolic potential of cells using two metabolic energy sources, namely mitochondrial and glycolysis energy pathways. It assesses the physiological changes that cells undergo regarding their surrounding environment, by elucidating the energy pathway cells choose to use for their energy demand and biosynthetic needs. The test gives insight about the mitochondrial dysfunction of the cells by simultaneously measuring these two energy pathways (102), looking at the basal state of cells and the state they transit into after they have been exposed to stressful conditions.

Cells were lifted and counted (as previously described). About 7.5 x 10^3 cells in 80 µl complete DMEM, were plated per well and they were left to adhere overnight in an incubator before treatment. Following incubation, cells were treated with 10 µl of each sunscreen active at various concentrations (*Table 2*). The microplate was left in an incubator for another 24 hrs. On the day of cell seeding, each well of the utility plate was filled with 200 µl of XF calibrant and the sensor cartridge was lowered onto the utility plate, submerging the sensors in calibrant. They were then placed in a non-carbon dioxide incubator overnight (to prevent evaporation of the calibrant).

Following the overnight incubation, the cartridge assembly was removed from the incubator. The sensor cartridge was lifted completely out of calibrant and utility plate, and immediately placed back. This was to eliminate any bubbles which may have formed overnight. Assay

medium constituted of Agilent Seahorse XF base medium, 2.5M Glucose, 100 mM Sodium pyruvate and 200 mM L-Glutamine, adjusted to pH of (7.4). The medium was then sterilised using 0.2 µm filter and incubated until ready for use (not more than 4 hrs). Thereafter, about 20 µl of the culture medium was removed from each well and cells were rinsed two times with 200 µl of assay medium, leaving 20 µl behind after each wash. Thereafter, 160 µl of the assay medium was added for a final volume of 180 µl. The plate was then placed in a 37 ^{0}C incubator without CO_2, for 45-60 minutes. Stressor mix stock compounds solution was prepared using oligomycin (63 nmol), carbonyl cyanide 4-(trifluoromethoxy) phenylhydrazone FCCP (72 nmol), which was topped up with assay medium. Thereafter, 20 µl stress mix was added on port A of the sensor cartridge, using a loading guide. Figure *12* shows procedure followed from isolating FFA fibroblasts, to culturing, treatment and tests performed post their treatment.

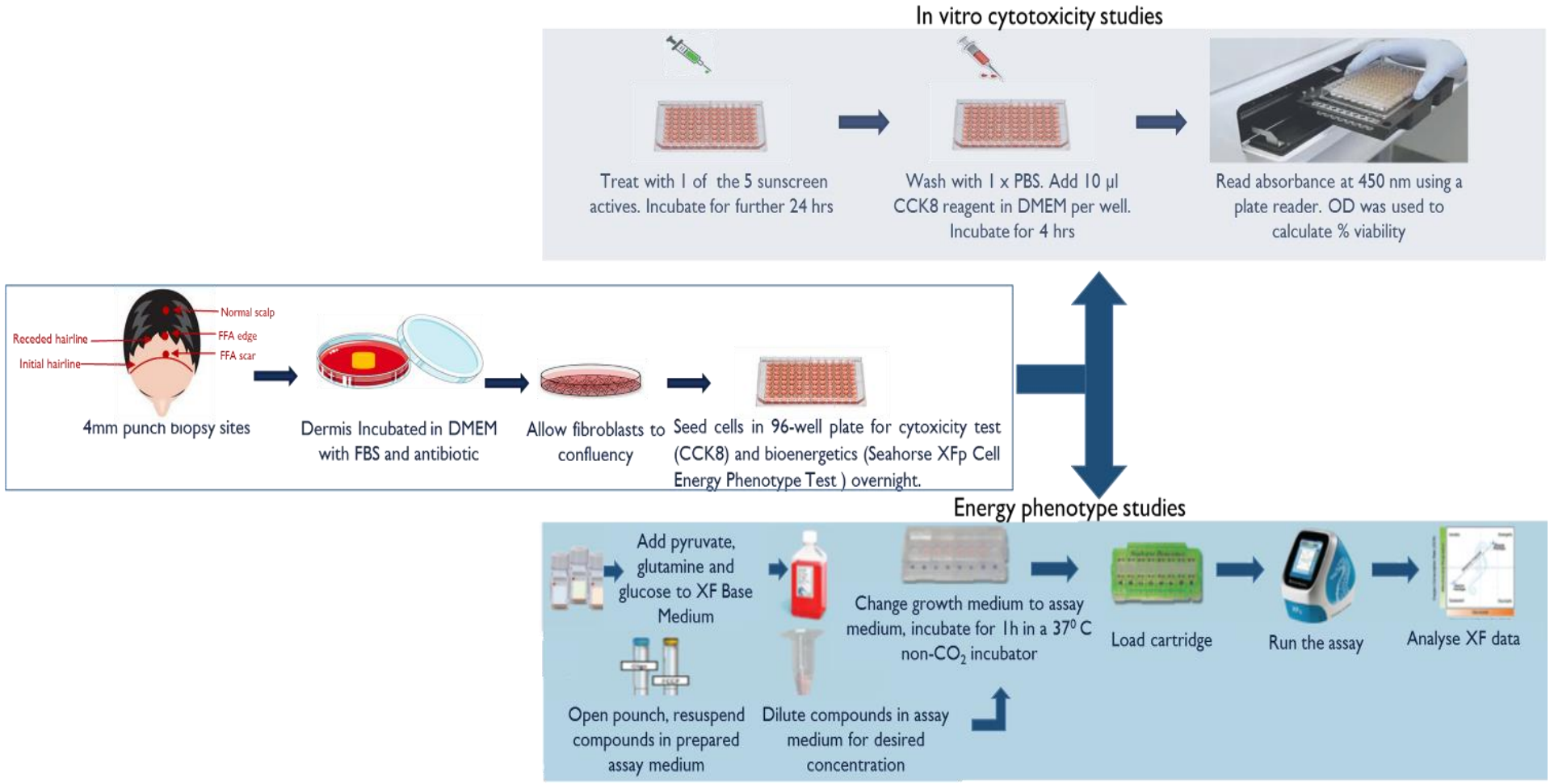

Figure 12 Flow diagram of sample collection, cells isolation and *in vitro* assays performed.

CHAPTER 3

3. RESULTS

3.1 MICROSCOPY

3.1.1 Scanning Electron Microscope and EDS

The presence of trace elements of interest (zinc and titanium), which are commonly used on sunscreens, were investigated on the FFPE sections from scalp biopsies isolated from FFA, LPP and TA individuals using SEM/EDS. Traces of zinc were detected on 33 % (3/9) of FFA cases, 9 % (1/11) cases of LLP and 0 % (0/5) cases for TA, however, no titanium was detected in any of the samples (Figure *13*). Traces of other elements unique to FFA cases were detected, and these are as follows: antimony (metalloid), plutonium (actinide), and arsenic (metalloid) and each were detected in varying cases. Lead was detected in 2 LPP only. On the other hand, two halogens (bromine – 3 cases and chlorine – 2 cases), and post-transition metal (indium – 1 case) were detected only in TA samples. Elements (potassium, promethium, nitrogen, terbium and carbon) as well as thulium, tin, molybdenum and hafnium seemed less in FFA than in LPP and TA cases. (**Appendix 1).**

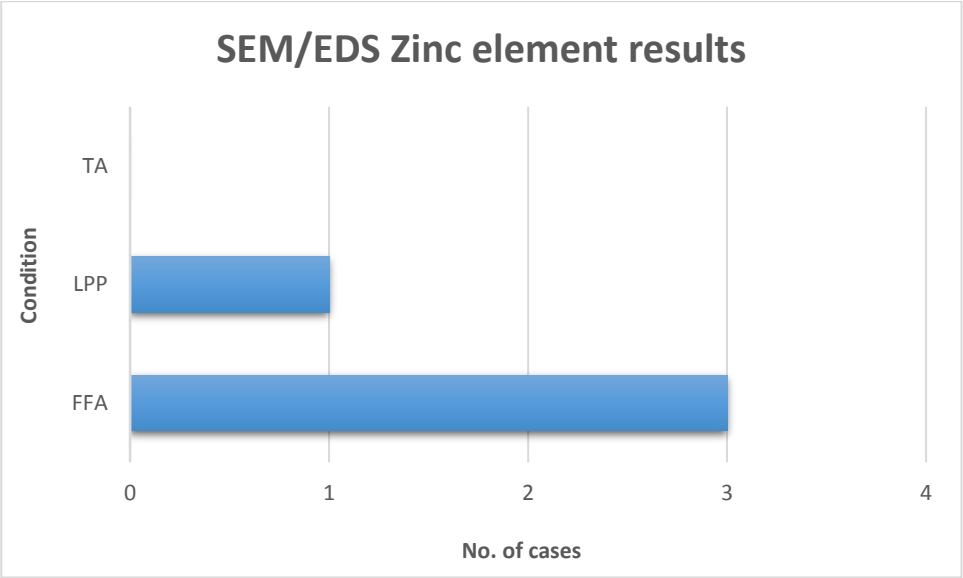

Figure 13 FFPE sections/cases of FFA, LPP and TA which the zinc element traces where detected on by SEM/EDS.

3.2 SPECTROSCOPY

3.2.1 FTIR-ATR

The aim of this part of study was to assess the potential presence of functional groups or molecules of the sunscreen actives on the FFA, LPP and TA archival tissues by means of FTIR. The ATR mode was used as a method of measurement. Eleven LPP, nine FFA and five TA FFPE scalp sections were analysed to determine the variation in the chemical fingerprint between the three conditions. The ATR-FTIR spectrum from FFA, LPP and TA tissue samples all looked similar in terms of the visible peaks (Figure *14*).

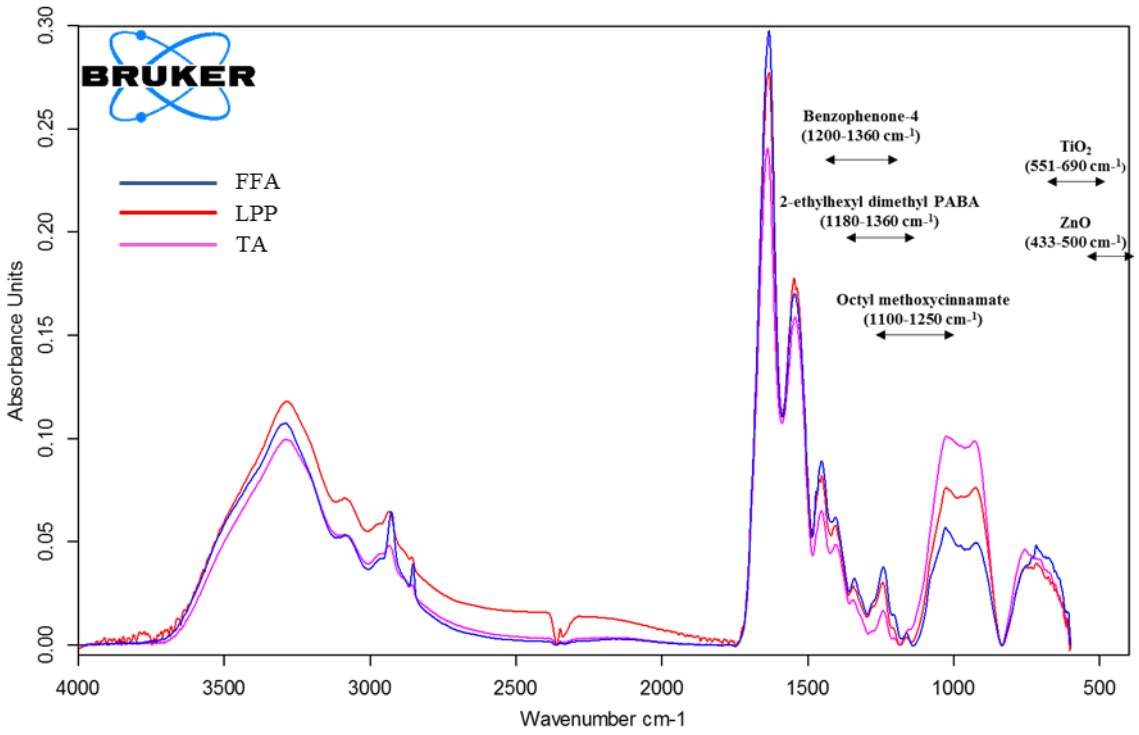

Figure 14 Representative spectra of one participant from each group, with the peaks of the 5 sunscreen actives used in the in Vitro study listed in the expected region. ATR-FIR spectral of FFA (blue), LPP (red) and TA (pink) FFPE scalp tissues.

Multivariate analysis software (SIMCA) that uses discriminant analysis (OPLS-DA) was used to further interrogate any inherent differences among the three hair loss conditions from the FTIR-ATR spectral obtained.

3.2.2 Principal Component Analysis (PCA) and Orthogonal Projections to Latent Squares Discriminant Analysis (OPLS-DA)

After obtaining the FTIR-ATR spectra of the three scalp conditions, the data was analysed using SIMCA. Fifteen spectra were collected from each FFPE scalp section of all the 25 sections as previously mentioned, resulting in a total of 375 spectra. Some of these obtained spectra had extremely low absorption values due to bad contact between the FFPE section glass slide and the ATR Geranium crystal. This resulted in exclusion of 68 spectra.

The PCA-X scores scatter plot (**Appendix 2**) of the combined data of all the three scalp condition groups was generated, to get an overview of the systematic separation patterns amongst the three hair loss conditions. There was no distinctive separation displayed between the three groups. The OPLS-DA models were then generated between the three groups. The first one constituted of all the three groups combined (Figure *15*) and the rest were comprised of two groups each, compared against each other, that is FFA vs LPP, FFA vs TA and LPP vs TA (Figure *16*).

The OPLS-DA model showed a better separation between the groups as compared to the PCA-X model. The FFA and LPP groups exhibited overlapping scores, but there was still a visible separation (R2 = 0.55) between them (Figure *16*A). On the contrary, comparisons between FFA vs. TA group (R2 = 0.92) and LLP vs. TA (R2 = 0.93) yielded a good separation between the hair conditions (Figure *16*C & E). An s-line plot was generated thereafter, to find the peaks that were attributed to the separation of the datasets (Figure *16*B, D & F). For the FFA vs LPP separation, a peak which contributed the most to the separation was found at 800 (cm^{-1}) wavenumber (Figure *16*B), whereas the separation peak between FFA and TA groups was found between 520-560 (cm^{-1}) wavenumber (Figure *16*D). There was no intense distinctive peak found responsible for the most separation between LPP and TA groups (Figure *16*F), however, slight separation was observed between the peak range of 1600-1620(cm^{-1}). All the peaks which were obtained on the s-line plot were attributed to compounds listed in **Appendix 2**, which included one of the compound strontium titanate, which contains one of our compound of interest titanium dioxide.

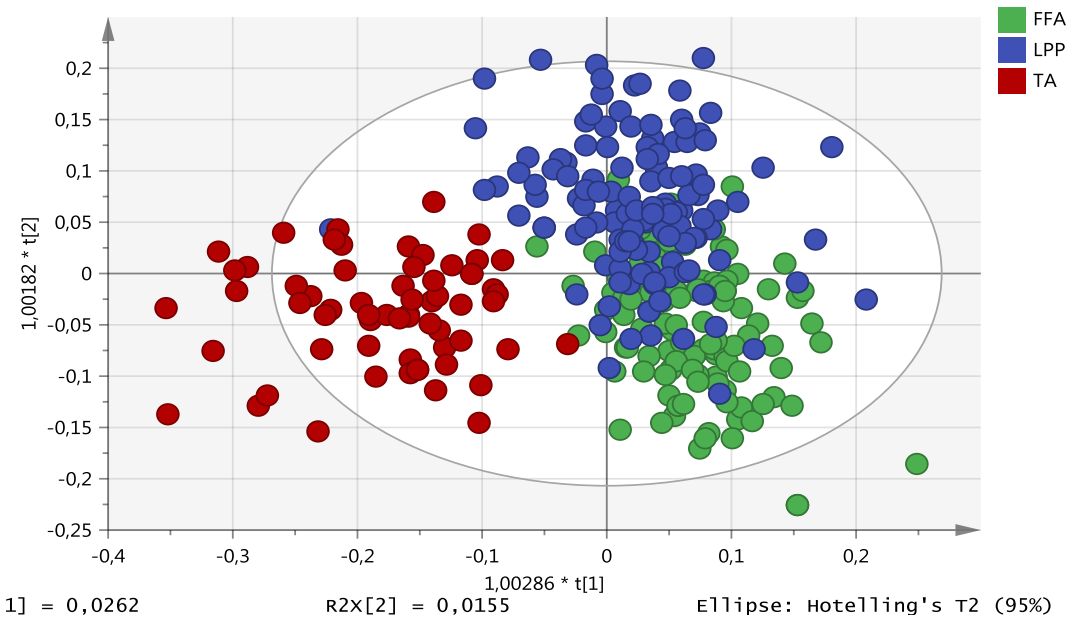

Figure 15 OPLS-DA scatter plot for the FFA, TA and LPP cases combined

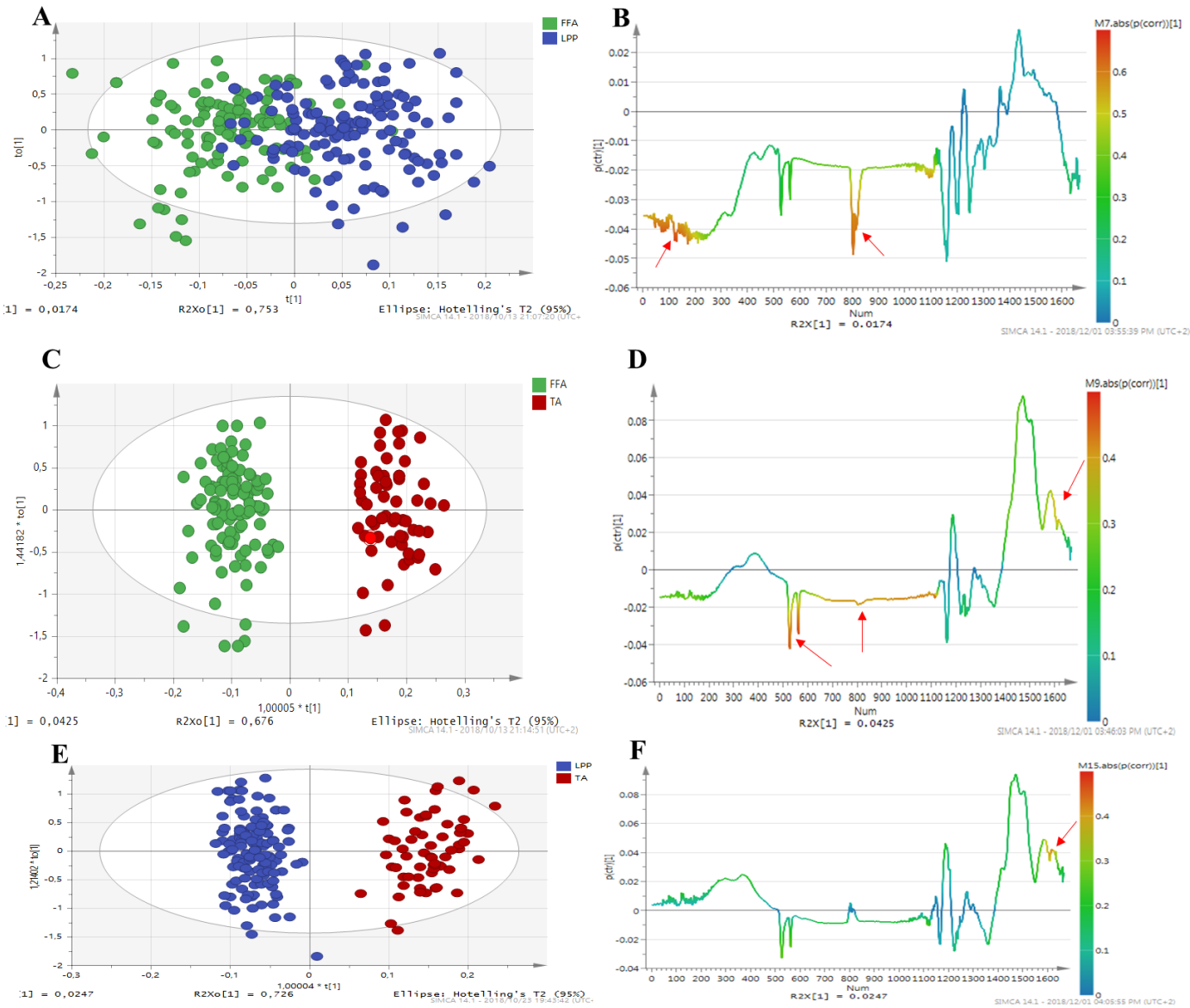

Figure 16 (A-B) OPLS-DA scores scatter and s-line plots of both the FFA, LPP and TA dataset combined. (A & B) shows separation between FFA vs. LPP, (C & D) represents separation between FFA vs. TA, whereas (E & F) shows the separation between LPP vs. TA. The red arrows show the peaks that attribute to the separation between the hair loss condition groups.

3.2 Evaluation of cytotoxicity of sunscreen actives using *in vitro* 2D monolayer models

Following detection of traces of elements of the sunscreen actives as well as their molecular detail from the FFA, LPP and TA archival tissues, we were interested in further investigating the potential cytotoxic effects of these aforementioned actives on both dermal and epidermal skin cells. To be more clinically relevant, we also obtained dermal fibroblasts from patients affected by FFA, with specific interest in the site/lesion-specific cytotoxic effects of these sunscreen actives. To do this, 4 mm punch biopsies were done on patients' scalp affected with FFA, these biopsies were cultured to allow for fibroblasts explants. Interestingly, 3 weeks in culture, fibroblasts explants from the active lesion (active hair loss) exhibited rapid growth in comparison to those from the fibrotic area **(**Figure *17***)** which was similar to that from the normal scalp**.**

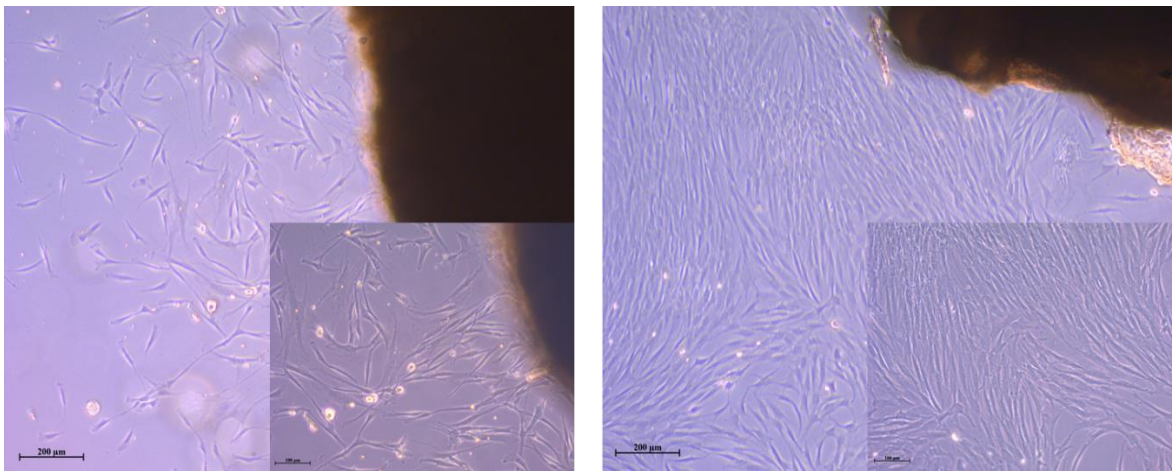

Figure 17 Images of fibroblast isolation culture from the FFA scalp punch biopsies, fibroblast isolated from FFA scar (left) and fibroblast isolated from FFA edge (right).

3.2.1 Evaluation of cytotoxicity of sunscreen actives on epidermal cells (keratinocytes)

The aim of the study was to evaluate the toxic effect of the sunscreen actives on the human epidermal skin cells by means of CCK 8 Titanium dioxide posed no cytotoxic effects (94%

viability from highest concentration) on epidermal cells (Figure *18*A), on the contrary, there was an increased concentration independent susceptibility to zinc oxide (37 % viability – highest viability percentage throughout all concentrations) compared to untreated keratinocytes (i.e viability three-fold lower) (Figure *18*B). Benzophenone-4 and 2-ethylhexyl dimethyl PABA (Figure *18*C and E) exhibited a statistically significant dose-dependent cytotoxic effect on epidermal cells (p=0.006 and p=0.0002 respectively). Whereas octyl methoxycinnamate showed a dose-independent cytotoxicity (Figure *18*D).

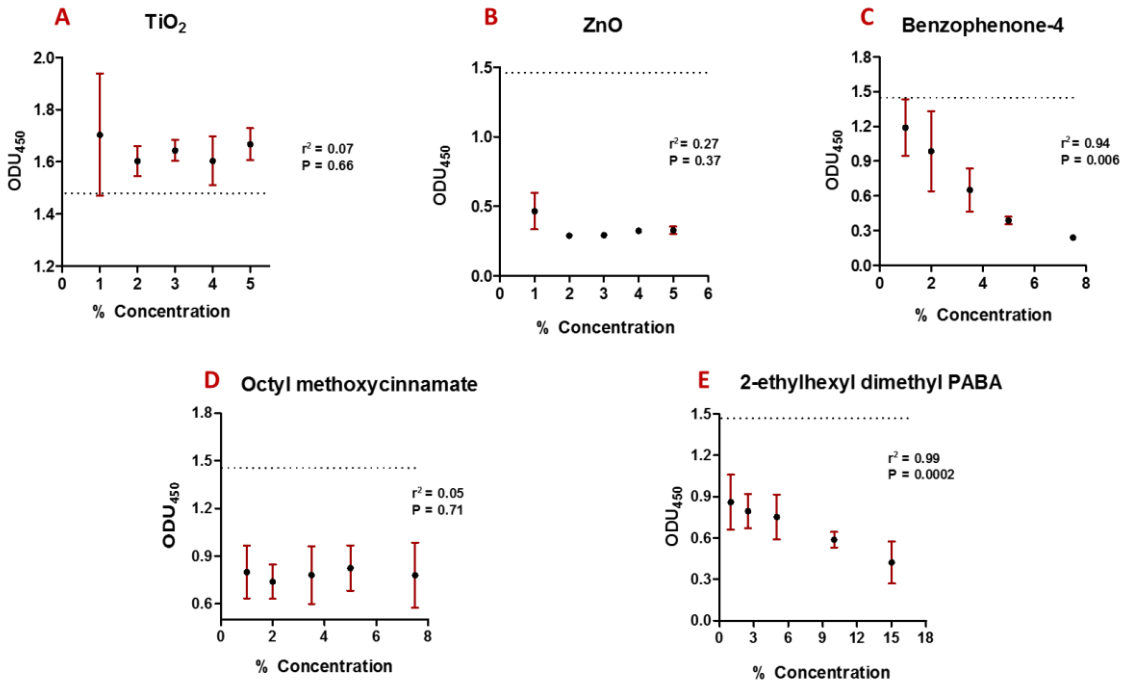

Figure 18 Correlation graphs of the viability of immortalized human keratinocytes 24 hours post treatment with sunscreen actives; untreated cells were used as reference for 100% viability of cells and it is presented by a horizontal dotted line.

3.2.2 Evaluation of cytotoxicity of sunscreen actives on site specific dermal fibroblasts

Following the evaluation of cytotoxic effect of the sunscreen actives on the keratinocyte cell lines, the same procedure was done on the site-specific primary scalp fibroblasts, particularly those of the FFA affected scalp.

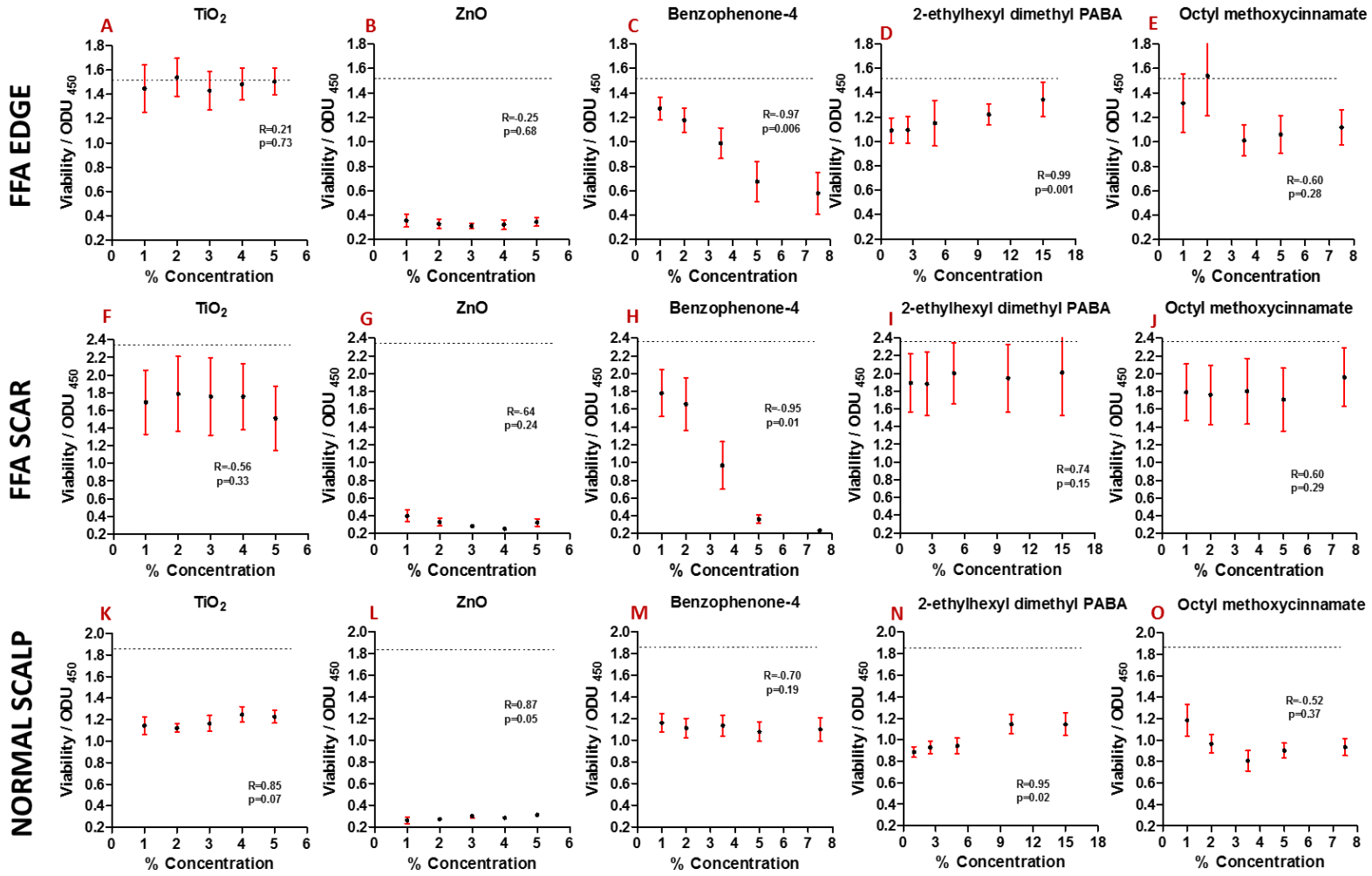

Figure 19 Correlation graphs of the viability of three different types of scalp fibroblast 24 hours post treatment with sunscreen actives, untreated cells were used as reference for 100% viability of cells and it is presented by a dotted line.

The normal scalp, FFA edge and scar fibroblasts, as observed from the cytotoxicity results of dermal cells post treatment with titanium dioxide, all the three-site-specific cell showed tolerance towards the titanium dioxide treatment (Figure *19*A, F and K). Whereas, the zinc oxide treatment showed a rather detrimental cytotoxic effect on all the three site-specific cell types (Figure *19*B, G & L), with normal scalp fibroblast exhibiting a significant correlation ($p = 0.05$) (Figure *19*K).

Benzophenone-4 showed a concentration dependent cytotoxic effect on both FFA scar and edge fibroblasts ($p = 0.006$ and $p = 0.01$, respectively) (Figure *19*C & H), except for the normal scalp fibroblasts (Figure *19*M) which maintained about 60% of their viability at all concentration levels. 2-ethylhexyl dimethyl PABA on the other hand, showed significant strong correlation between its concentration levels and the viability of the FFA edge ($p = 001$) and normal scalp fibroblasts ($p = 0.02$) (Figure *19*D & N). There was a relatively good correlation ($r^2 = 0.74$) between the viability of FFA scar fibroblasts and 2-ethylhexyl dimethyl PABA concentration levels, although the correlation was insignificant (Figure *19*I). The treatment with octyl methoxycinnamate showed dose-independent cytotoxic effect on all the three site-specific cells types (Figure *19*E, J & O).

After determining the toxic effect of the different sunscreen actives at their varying concentrations levels on each previously mentioned scalp fibroblasts, the three cell types where then compared to one another regarding their susceptibility to the sunscreen actives at their different concentration levels. There was no significant difference among the viability of the cell types before treatment (Figure *20*A) and so was post the titanium dioxide (Figure *20*C) and zinc oxide (Figure *20*E) treatment.

However, there was a significant difference on the overall viability of the three cell types, post treatment with 2-ethylhexyl dimethyl PABA ($P = 0.0096$) (Figure *20*D) and octyl methoxycinnamate ($P = 0.0191$) (Figure *20*F). In addition, significant difference ($P<0.0001$)

was also observed from among the viability of the three cell types, post benzophenone-4 treatment (Figure *20*B). The FFA scar fibroblasts accounted for more of this observed significant difference in the cells' viability, more especially between treatment at the highest (7.5%) and lowest (2 %) concentration levels.

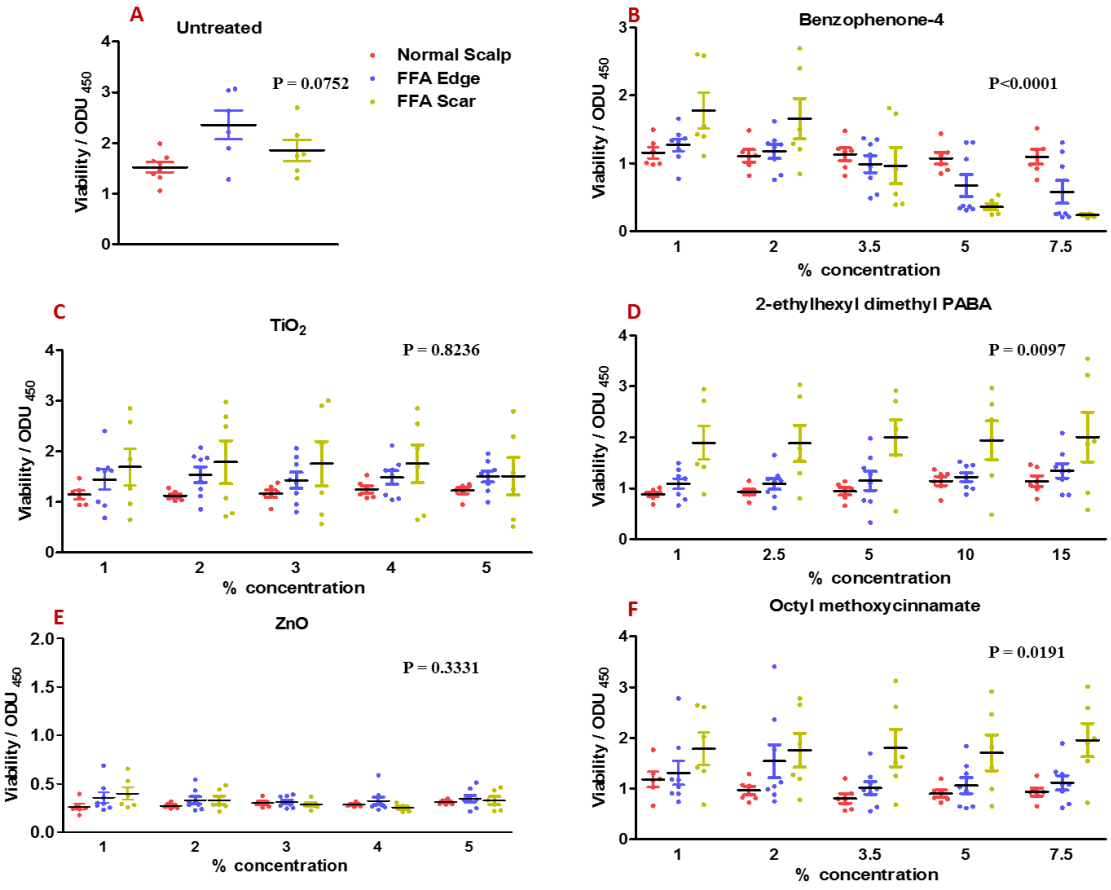

Figure 20 Comparison of three different types of scalp fibroblasts viability post treatment of different sunscreen actives, at their different concentration levels.

3.2.2 Extracellular flux energy phenotype analysis on epidermal and dermal cells post sunscreen actives treatment.

After the evaluation of the cytotoxic effect of the sunscreen actives on both the keratinocytes and scalp site-specific fibroblasts, we saw cytotoxicity perturbations. Therefore, we sought to further investigate whether these perturbations are metabolic. To achieve this,

extracellular flux analysis was used to measure the energy phenotype of the cells post treatment with the actives.

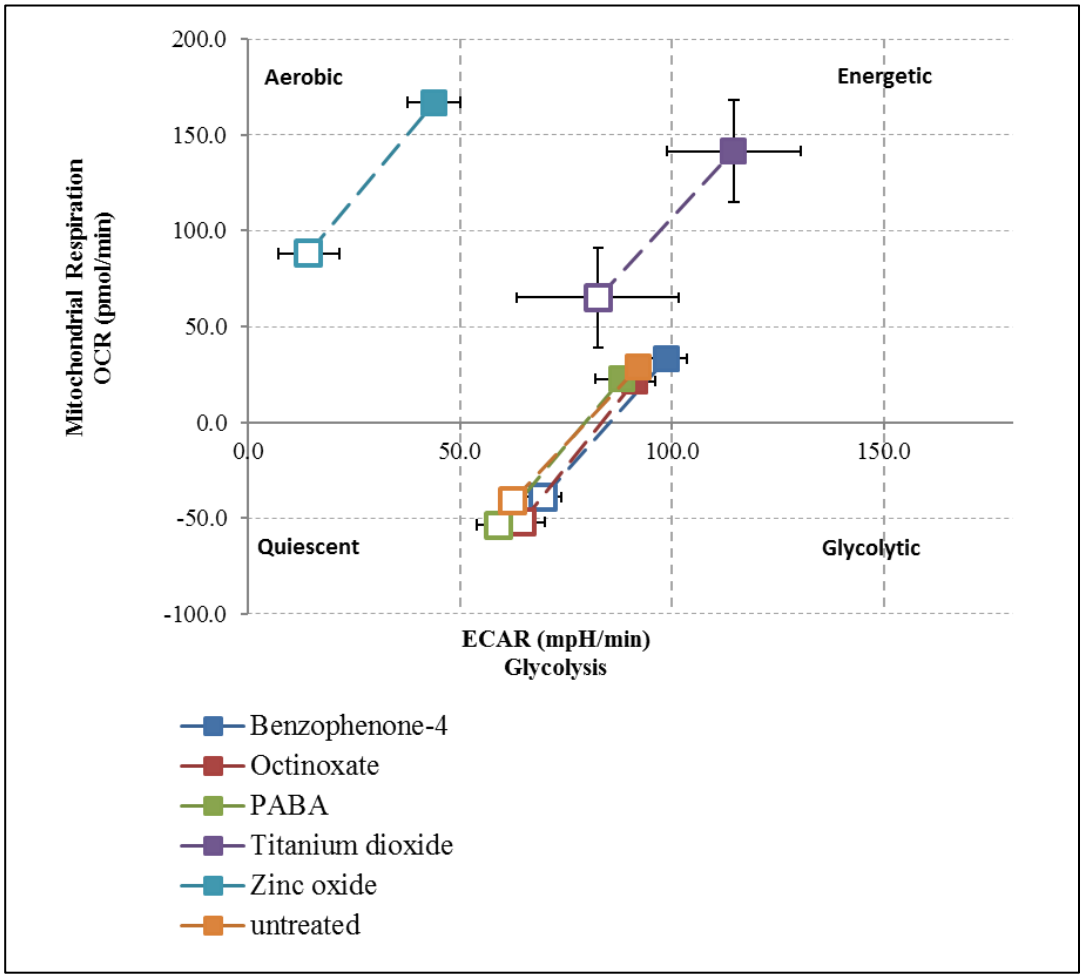

Figure 21 Energy phenotype map of keratinocytes post 24 hours sunscreen actives treatment.

Both the epidermal and dermal cells were treated with the sunscreen actives individually, for 24 hours and their energy phenotype switch was measured, to evaluate the effect of the sunscreen actives on their energy pathway. The dermal cells exhibited a quiescent state post treatment with sunscreen, except for the ones which were treated with zinc oxide and titanium dioxide (Figure *21*). After being introduced into a stressful environment, their energy phenotypes switched to a glycolytic state and the ones which were treated with zinc oxide and titanium dioxide moved towards an energetic state.

On the other hand, untreated FFA scar, FFA edge and normal scalp fibroblast were shown to be glycolytic, especially the FFA edge cells. After being stressed, the normal scalp and FFA edge cells moved towards an aerobic state, whereas the FFA edge cells switched to an aerobic/energetic state (Figure *22*). Following 24 hours treatment with benzophenone-4, normal scalp cells switched from a glycolytic state towards a slight quiescent state, whereas FFA scar and FFA edge cells moved towards an aerobic state (Figure *23*). Moreover, zinc oxide treatment switched all the three site-specific fibroblasts energy pathway from a glycolytic to a quiescent one (Figure *23*). Whereas, titanium dioxide treatment caused them to switch from a glycolytic to an energetic state (Figure *24*).

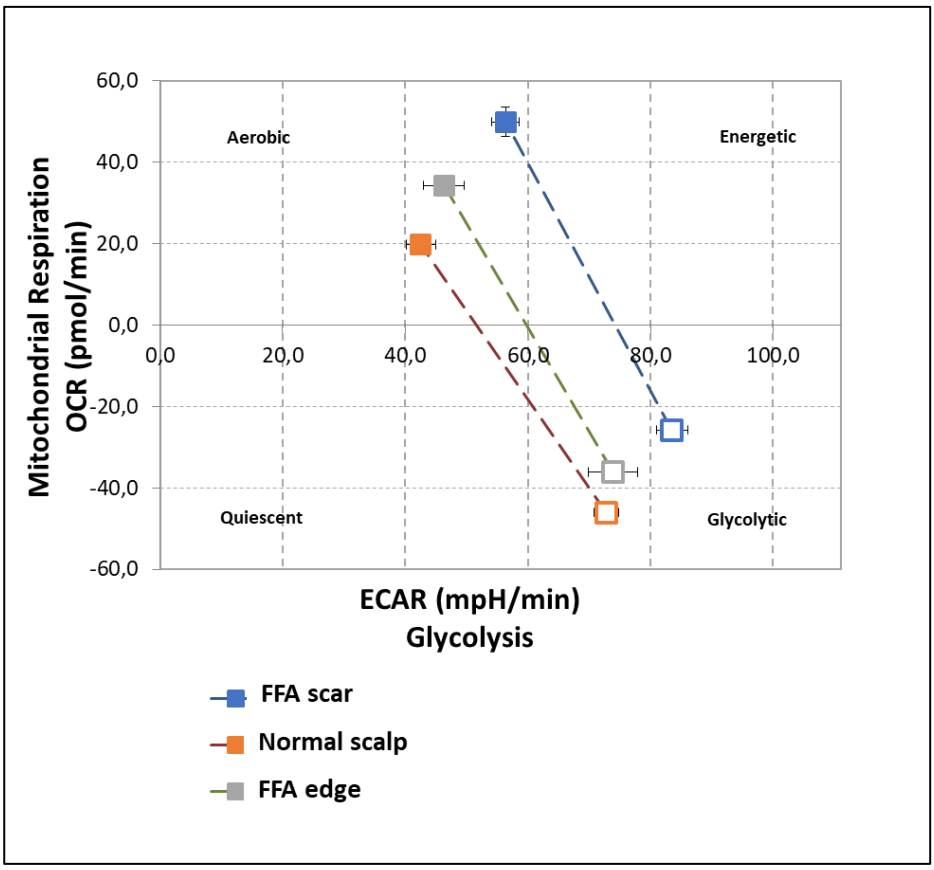

Figure 22 Energy phenotype map of untreated primary fibroblast isolated from FFA scar, FFA edge and normal scalp tissue.

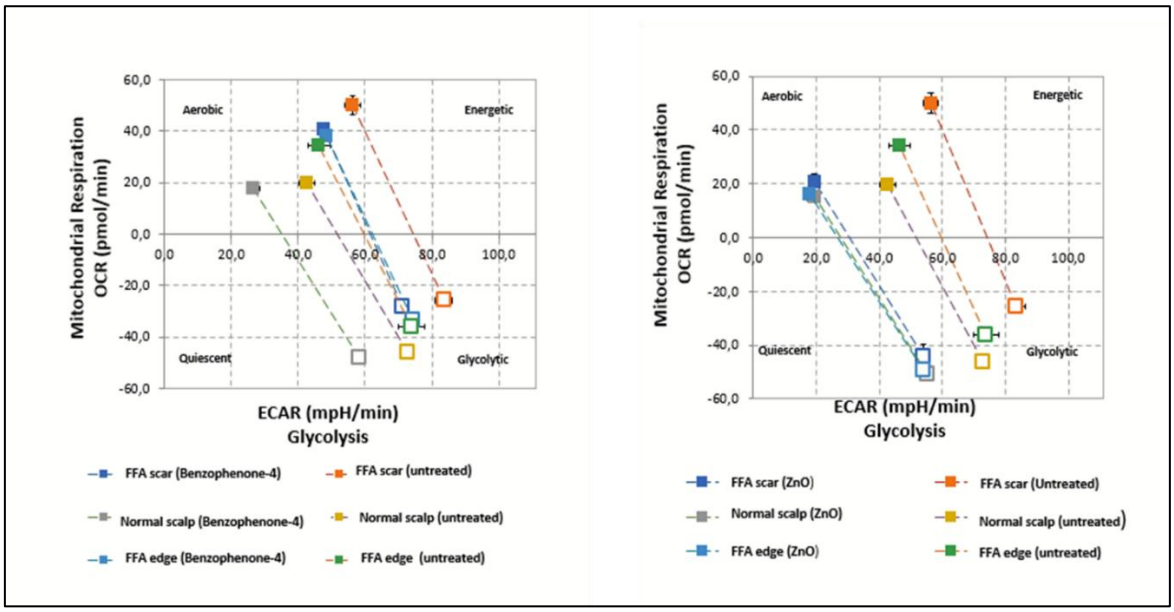

Figure 23 Energy phenotype map of primary fibroblast isolated from FFA scar, FFA edge and normal scalp tissue before and after 24 hours treatment of zinc oxide and benzophenone-4, respectively.

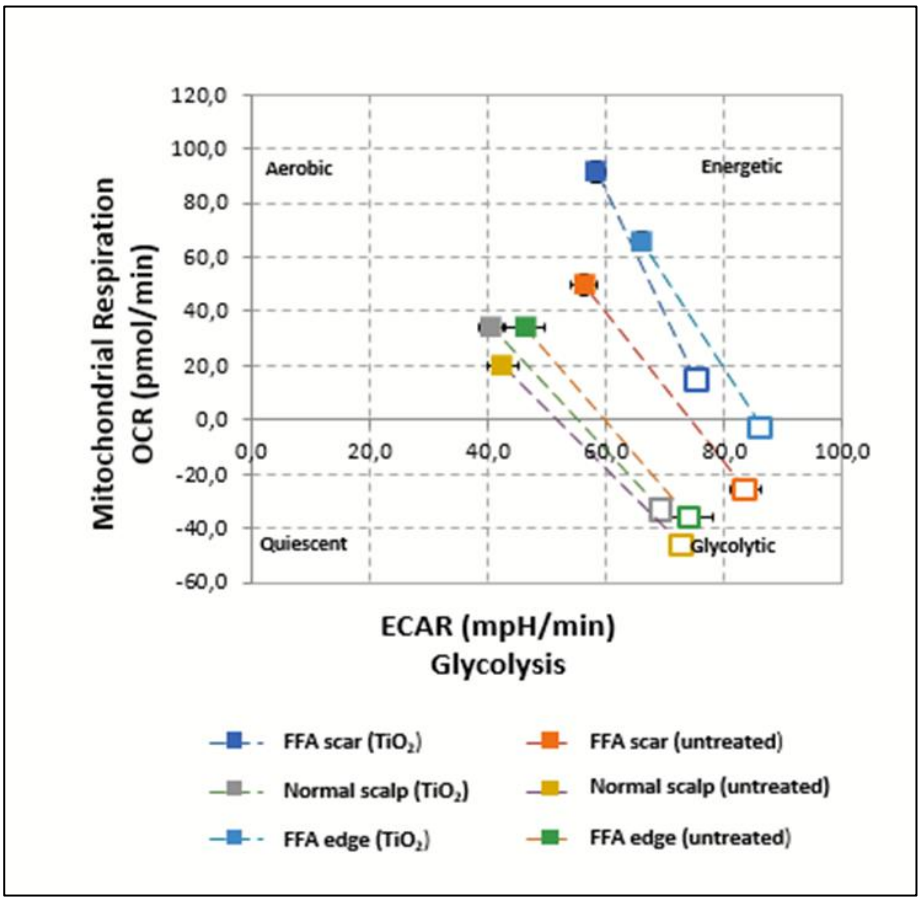

Figure 24 Energy phenotype map of primary fibroblast isolated from FFA scar, FFA edge and normal scalp tissue before and after 24 hours treatment of titanium dioxide

CHAPTER 4

4.1 GENERAL DISCUSSION AND CONCLUSION

Frontal fibrosing alopecia is an irreversible scarring hair loss condition which to date, no exact cause for it has been identified (37&77&103). There has been an increase in its incidence over the past years (15&73&104-106), and this has sparked an interest within the medical and scientific communities. Hair loss such as FFA can be really disfiguring and cause a serious psychosocial stress on the affected individuals, especially in women (107&108).

With the increasing incidences and little being known about aetiology of FFA, only speculations have been made regarding its causative factors, one of such raised suspicion it is the environment (51&109). It has been suggested that there could be an environmental factor (s) playing a role in the etiopathogenesis of FFA and one of such factors is the use of sunscreen (17&109&110). There has been a paucity of experimental work done to validate the possibility of an association between FFA and sunscreen actives, except for a study by Brunet-Possenti, Deschamps (111) and Thompson, Chen (23), which reported the presence of titanium particles in a hair shaft of an FFA patient. All other studies that have reported possible association between FFA and, sunscreens and leave-on facial creams are questionnaire-based studies.

This current study aimed at looking into the possibility of an association between FFA and sunscreens, using in-vitro molecular studies and high-end microscopy instrumentation. To achieve this aim, four techniques were explored, this included cytotoxicity assay, extracellular flux bioenergetics assay, microscopy and spectroscopy analysis. Both the fresh and archival FFA tissues were investigated using the previously mentioned techniques. The archival tissues were investigated using both the microscopy and spectroscopy analysis, to

detect the potential elemental presence of commonly used sunscreen actives. Whereas, fibroblast cells were isolated from fresh clinical biopsy tissues and their sensitivity to sunscreen actives was investigated using cytotoxicity and extracellular flux bioenergetics assays.

4.1.1 SEM/EDS analysis on the scalp archival tissues of FFA, LPP AND TA.

SEM/EDS analysis was used to detect the presence of the elemental form of sunscreen actives, more especial the metal ones such as zinc and titanium on the FFA archival tissue sections. The archival tissues of LLP and TA were used as control. Interestingly, more FFA tissues sections had the presence of zinc, which is one of the commonly used sunscreen (UV filter) active ingredients (53) as compared to the controls. A similar finding was reported by Brunet-Possenti, Deschamps (111). Whereby, titanium, which falls within the same category of sunscreen blockers as zinc, was detected in the hair shaft of a patient affected by FFA.

However, with EDS being more of a qualitative than a quantitative analysis, it is quite difficult to conclude whether the detected zinc in the FFA scalp sections was an exogenous or endogenous. Moreover, elements such as arsenic, tin, lead and thallium were also among the detected elements of all the scalp sections from the three different hair loss conditions. These elements have been implicated in the disruption of the normal ongoing hair cycle, resulting in hair loss (112-115). Arsenic, antimony, lead and thulium are considered heavy metals and they are part of the thousands substances which have been banned from the cosmetic industries by the European Union Scientific Committee on Consumer Products (Annex II), due to their toxicological properties (116-118). Interestingly, Bocca, Pino (116) reported arsenic's an affinity for keratinized structures such as hair and nails, which leads to detrimental effects such as alopecia. Therefore, its detection on one of the FFA samples it is not farfetched. Aluminium (light metal) is still currently used in the cosmetic industries, but it is considered harmful when it is in excessive amounts (117). Even though banned, some

of these metals are still found on some cosmetic products, as contaminants. All the elements that were unique or higher in each hair loss condition, their source and uses are listed in Table *5*.

Table 5 Traced elements from the FFA, LPP and TA archival scalp biopsies sections by SEM/EDS (119)

Element	Natural Source	Uses
Antimony	Its natural occurrence it is found in the environment (makes up approximately 0.00002% of the earth's crust) and it is rarely found as a free element in nature. It is often generated from the stibnite and valentinite ores.	• Its pure form it is used to make diodes and infrared detectors. • Its alloys are used in batteries and low friction metals manufacturing. • Its compounds are used in the making of flame-proof materials, glass, paints and ceramics enamels. • The ancient Egyptians used antimony (stibnite form) for black eye make-up. • Treatment for parasital infections.
Arsenic	It is naturally found in small quantities on earth. The common occurrence places are the soil and minerals. It can also be transferred through air, water and land by wind-blown dust and water run-offs.	• Make a special type of glass. • Used as a wood preservative. • And in semiconductor (gallium arsenade).
Bromine		

	It is found in many inorganic substances and does not occur as a free element in nature as it is highly reactive.	• Used in the manufacturing of fumigants, dyes, flame-proof agents, pharmaceuticals. • For water purification. •
Carbon	Most quantities occur in compound forms. It is naturally widely distributed and approximately makeup about 0,032% of the earth's crust.	• Graphite form is used for high-temperature crucibles, pencil tips, and dry cell. • Used as black fume pigment in vehicle's rims and printing ink. Its compounds are used for various purposes such as carbonation is sodas, fire extinguishers and as dry ice for biological samples preservation.
Chlorine	It naturally found in combination with other elements, mostly in the form of sodium chloride, and other forms such as carnallite and sylvite. Its components make us most of the salt dissolved in the oceans (chlorine ions approximately take up 1.9 % of the seawater's mass).	• Mostly used as a water purification compound and disinfectant.

Hafnium	It does not naturally occur in a pure form on earth. It is usually generated as a by-product of zirconium.	• Together with its high-temperature alloys, are used for control rods in nuclear reactors and nuclear submarines. •
Indium	It is an element which is not widely distributed in the environment and cultivated soils are believed to be a great source of it. It can also be produced as a by-product of smelting lead sulfide and zinc ores.	• Used as a mirror surface that is corrosion-resistant. • Foils made from indium are used to inspect the inside of nuclear reactors. • Used in the manufacturing of low-melting fusible alloys.
Krypton	It is one of the rarest atmospheric gases, but it is estimated that about more than 15 billion tonnes of it circulating on the planet.	• Used for filling up electric lamp bulbs and used for various light lamps such photographic projection lamps.

		• Used for the detection of leads in sealed containers. • Detection of abnormal heart openings in the medical field.
Lead	Pure lead is seldom found in nature. Its current source is found in ores from a combination of metals (zinc, and silver). It is also usually found in combination with sulfur.	• Manufacturing of lead-acid car batteries, cables, ammunition, and sports weight equipment. • Pigmenting compound in ceramic glazes. • Radiation shield on computer and television screens.
Molybdenum	Earth crust and oceans.	• Used in alloys, electrodes, and catalysts. Its powder is used for microwaves and circuit inks
Nitrogen		

	Its molecules naturally occur in the air; however, the nitrates and nitrites are found in water and soil.	• It is mostly used in the manufacturing of ammonia. • Also used as a fertilizer. • Liquid nitrogen is used as a freezing agent for the transportation and preservation of biological samples and food products. •
Plutonium	Its traces are naturally found in uranium-rich ores and another great source of it is the nuclear weapons.	Used for the manufacturing of modern nuclear and radiological weapons.
Potassium	Its natural occurrence is found in the earth's crust and another great source of it is food products such as vegetables, fruits, meat, and milk.	• Majority of it is used in fertilizers and the rest is used for the manufacturing of potassium hydroxide. • Its components are used for various purposes such as glass manufacture, liquid soaps, and pharmaceuticals.

		•
Promethium	Naturally occurs in the earth's crust in small quantities and in some uranium ores.	• Mostly used for research purposes. Used in nuclear batteries, watches and light source for signals.
Terbium	It is one of the earth's rarest element and it is never found in nature in its pure form, but it is contained in many minerals. The ores it is constituted in are monazite, bastnaesite, and cerite.	• Is has few commercial uses, as it is one of the rare and expensive elements. One of its few uses includes manufacturing of lasers, semiconductor devices and a stabilizer of fuel cells which operate at high temperature.
Thulium	It cannot be found naturally found in a pure form, but it is found in combination with other minerals in small quantities. It is usually extracted from monazite.	• It is a rare and expensive element; therefore, it has a very few commercial uses. Apart from research use, it can also be used as a radiation source in X-ray devices. •
Tin		

	It is one of the abundant elements in the earth's crust. However, it does not occur solely but must be extracted from various ores.	• Used to coat cans which are widely used for food preservation. • Manufacturing of tin foils used as food wrap. • Some of its alloys are used for ceramics and in gas sensors
Zinc	Zinc is a common natural occurring element and the common place it is naturally found are air, water and soil.	• Used for galvanizing iron and preparing some alloys. • Used in printing equipment, cosmetics and plastics. • Possess some anti-oxidant properties for the protection of the skin and body muscles.

Limitations and future prospective studies:

This study had a small sample size, which makes it difficult to conclude whether there is a direct link between the elemental zinc detected on some of the samples to the hair loss condition. Moreover, there was no information regarding the sunscreen use history of the patients from which the archival tissues were biopsied from. Therefore, before a definite conclusion could be made regarding the presence of zinc on the FFA scalp sections, a bigger sample size with a known history of sunscreen use, would be required. In addition to that, a more sensitive quantitative technique such as the Inductively Coupled Plasma Mass Spectrometry (ICP-MS) could be used. It could be more ideal on ruling out whether the detected elements on the scalp sections are in their normal expected quantity found in the body's biological system or whether the detected amounts are abnormal.

However, the mere fact that elemental zinc was detected in more FFA samples as compared to its controls, being LPP and TA, such results cannot be merely ignored. They rather should be treated as a compass which will point us to a better direction in attempting to elucidate this suspected association between FFA and sunscreen actives.

4.1.2 FTIR/OPLS-DA analysis of the scalp archival tissue of FFA, LPP AND TA.

One of the objectives of this study was to elucidate the chemical fingerprint of the archival scalp tissue sections. The ATR-FTIR spectrum from FFA, LPP and TA tissue samples all looked similar in terms of the visible peaks (Figure *14*). FTIR spectral were analysed using a discriminant technique called OPLS-DA. The OPLS-DA enabled us to analyse the trends among the three conditions and how they separate from one another, given that they are different clinical hair loss conditions (2).

As expected, there was an overlap between FFA and LPP data points, this could be due to the fact that there is published evidence (103&120-122) suggesting that they are clinical

variants, as they share histopathological similarities. There was clear separation of data points observed when comparing FFA versus TA and LPP versus TA. Their fraction of variation (R2) according to the OPLS-DA analysis is R2 = 0.550 as compared to FFA vs TA (R2 = 0.933) and LPP vs TA (R2 = 0.934). Therefore, the two lymphocytic hair loss conditions are similar which is consistent with them being clinical variants, given that the discriminant method only managed to discriminate them against each other by only 55 %. The peak which contributed the most to the separation between FFA and LPP was found at a wavenumber, 800 (cm^{-1}), which it is attributed to lithium molybdate and this corresponds with the SEM/EDS data whereby an element Molybdenum was detected in some of the LPP FFPE samples (**Appendix 1**).

When FFA and LPP were compared against TA, which is a non-scarring form of hair loss, the R2 of both comparisons show good separation (92 % and 93 % respectively). Although no exact molecular detail for specific sunscreen actives on the scalp sections were detected, strontium titanate was a significant contributor to the separation between FFA and TA. Strontium titanate was present but not a significant contributor to the separation between LPP vs. FFA or LPP vs. TA. Strontium titanate is a perovskite material that is used a diamond simulant and electricity (123-125). Although strontium titanate contains the compound titanium dioxide, we could not find evidence of its use as a cosmetic ingredient or that it released titanium dioxide that could come into contact with human skin. The observation of the separation trends between the hair loss conditions was an interesting discovery, as it confirms the suggestion that FFA and LPP are clinical variant of one another.

Limitations and future prospective studies:

Some spectra had to be excluded before OPLS-DA analysis was performed, as mentioned in (**3.2**). This was one of the setbacks of the study, as the excluded spectrum could have yielded a more insightful information regarding the samples. The excluded spectra were the

ones which had a low absorption, due to a bad contact between the tissue sample and the FTIR-ATR crystal.

A limited sample size was one of the constraints which were encountered, as a bigger sample size could have enabled us to discover more peaks which contributed the most to the separation between different three hair loss conditions. Therefore, increasing our chance of detecting potential molecular fingerprints of some of the sunscreen actives. In addition, there were no precise background history regarding cosmetic use from the patients whose scalp samples were used for this study. Such information could have helped in identifying which samples were more likely to have traces of the functional groups of some of sunscreen actives.

More research needs need to be conducted, preferably with a larger sample size to obtain a more conclusive result regarding the chemical fingerprint of this hair condition. In which case, more evaluation could be made to determine whether a more significant chemical fingerprint could be identified. This could be used as one of the diagnostic tools in the analysis of the disease progression. Whereby, a chemical fingerprint of an actively progressing FFA is compared to the one which has halted and determine if there is any significant difference between their chemical fingerprint.

4.1.3 Evaluation of cytotoxicity of sunscreen actives using *in vitro* 2D monolayer models

There was not much insight found from the results obtained, after tracing some elements which were implicated on the hair loss condition, with the use of SEM/EDS and FTIR-ATR/OPLS-DA, from the scalp archival tissues of FFA, LPP and TA. Therefore, we decided to explore more techniques in attempt to prove our study hypothesis. To achieve this, we evaluated human keratinocytes (epidermal cells) and FFA fibroblasts (dermal cells) which were isolated from fresh scalp tissues which were affected by FFA. Normal scalp fibroblasts

were used as healthy controls and were obtained from the unaffected scalp region (vertex) of the FFA patients' scalp. This region was chosen as the healthy lesion, because it is a region which is rarely affected by FFA and it has a normal hair density present. Five commonly used sunscreens actives were used to carry this out for both the chemical and physical sunscreens. Although, some sunscreen actives showed a distinctive cytotoxic effect on the cells, some exhibited a negligible cytotoxic effect on the cells.

4.1.3.1 Cytotoxic effect of physical sunscreen actives on the cells

Zinc oxide and titanium dioxide were two actives out of the five used in the study, which were used for the cytotoxic analysis. They are categorially classified as physical sunscreen blockers (126). Moreover, they have been implicated in a number of biological disruptions such as genotoxicity and endocrine disruption (55), and their recent formulation properties such as nano-size has been under scrutiny, with their safety in terms of skin permeation questioned (21&54).

Although, titanium dioxide and zinc oxide are classified as mechanical sun blockers, there seems to be marked differences in their cytotoxic effects. From the obtained cytotoxicity results, zinc oxide exhibited a more detrimental cytotoxic effect on all the cells' viability as compared to titanium dioxide. Similar findings were reported by other studies (55&127-129). Whereby, *in vitro* cytotoxicity studies were performed on other cell types (immune cells) to investigate the cytotoxicity of these two metal oxides and zinc was found to be the most toxic on the cells as compared to titanium dioxide. The data obtained indicate a dose-independent cytotoxic effect on zinc oxide irrespective of the lesional site. On the contrary, we observed site-specific susceptibility of cells post treatment with titanium dioxide, wherein normal scalp-derived fibroblasts were more susceptible as compared to those derived from the edge and scar respectively.

4.1.3.2 Cytotoxic effect of chemical sunscreen actives on the cells

We then evaluated the cytotoxicity of the chemical sunscreen actives (octyl methoxycinnamate, 2-ethylhexyl dimethyl PABA and benzophenone-4). These have been implicated in endocrine disruption and genotoxicity on various biological components (130-133).

Overall, keratinocytes and normal scalp fibroblasts were shown to be the most susceptible to the chemical actives treatment as compared to the FFA-derived cells. There is a distinct difference between the susceptibility of all the three site-specific scalp fibroblasts, which is what we had hoped for. FFA scar fibroblasts showed the greatest resistance, whereas FFA edge and normal scalp fibroblasts showed susceptibility. This may be due to the hypoxic microenvironment (fibrous tissue), from which they were derived that rendered such cells more adaptive to unfavourable conditions. A study evaluating the cytotoxic effects of photodynamic therapy (PDT) on site-specific keloid-derived fibroblasts (a fibrotic disorder) also showed varying susceptibility to the aforementioned therapy (134).

4.1.4 Extracellular flux energy phenotype analysis on epidermal and dermal cells post sunscreen actives treatment.

After evaluating the cytotoxicity of the five sunscreen actives previously mentioned, distinct cytotoxic effects were observed among the three-site-specific scalp fibroblasts. This finding led us to further evaluate what brought about such differences, hence cellular energy phenotype analysis was performed on the same cells 24 hours post treatment with the sunscreen actives.

The test was initially performed on the human keratinocytes. Our study demonstrates that chemical actives induces a negligible energy phenotype switch of the keratinocytes, with a slight shift from a quiescent towards a glycolytic state. A similar trend was observed on the

healthy cells which had no treatment, which suggests that organic actives did not alter the energy phenotype of the cells.

On the contrary, physical actives induced a noticeable energy phenotype switch of both epidermal and site-specific dermal cells. This observation shows that there are some energy metabolic changes that these nano-metal oxides may cause in the cells. All the scalp fibroblast exhibited a baseline glycolytic energy phenotype. Upon stress, the FFA scar fibroblast shifted towards an energetic state upon stress, whereas FFA edge and normal scalp fibroblast shifted towards an aerobic state post titanium dioxide and benzophenone-4 treatment.

Zinc oxide resulted in the energy phenotype change in all site-specific scalp fibroblasts, wherein the cells' energy phenotype changed from the glycolytic to the quiescent state. Such a quiescent state may be because of cell death, since our cytotoxicity studies demonstrated significant cytotoxic effects of this physical sunscreen active.

Evaluation of energy phenotype of untreated site-specific dermal cells showed that FFA scar fibroblasts displayed a higher metabolic potential rate (**Appendix 6**) as compared to both edge and normal fibroblasts. This is interesting as the data is in line with our cytotoxicity results, whereby such untreated cell showed a higher viability.

To our knowledge, no studies have previously evaluated the cellular bioenergetics using patient-derived in vitro monolayer culture models. However, further research is needed to investigate specific molecular mechanisms underlying such changes.

In essence, this study may suggest as reported by Aldoori, Dobson (17) that the use of these sunscreen actives may not necessarily be the cause of FFA, but they merely play a role in its aggravation by inducing an allergic response which trigger an inflammatory destructive reaction to the hair follicle.

Limitations and future prospective studies:

Working with primary fibroblasts was challenging, because once they passed the passage number 3, they were no longer suitable for use for metabolic studies such as cells' viability and bioenergetics due to change in physiological properties. This limited the number of experiments carried out. For future studies, more samples can be used to allow more isolation of cells from the tissue, so that a great stock of cells can be cultured, enabling more experiments to be carried out to find more conclusive results than the ones found in this study. In addition, the other limiting factor was that the normal scalp region fibroblast was obtained from the unaffected scalp area on the FFA participants. As no specific measure was made to determine if the area was indeed unaffected or not, regardless of the normal hair density present, which could influence the results.

Another limitation of the study was that there was quite a limited background history regarding cosmetic use from the patients whose scalp samples were used to derive FFA primary fibroblasts. As the patients could not recall well and be specific enough about the products they were using during the onset of the disease and the years after diagnosis, the only demographic data obtained from the patients is as documented in Appendix 7 (***Table 10***). Moreover, even FFA derived fibroblasts cell-line can be developed, which would allow adequate passage numbers to culture cells and do adequate experiments on them without them losing much of their physiological properties.

4.2.1 CONCLUSION

Since the first report in postmenopausal women by Kossard, in 1994, the number of FFA reported cases initially remained low. However, in the last decade there has been an exponential increase in cases which include younger women and even men, with the largest study reporting cases of 355 patients. Further, there has also been an exponential increase in

both the number of cosmetic products incorporating nanotechnology-based ingredients and in the number of publications expressing safety concerns related to these products. The FTIR spectra overlap between FFA and LPP is consistent with current clinical understanding of this spectrum of alopecias. The separation between FFA and TA contribution by a compound that is biochemically linked to titanium dioxide is a clue that needs further investigation. The higher presence of zinc traces in FFA samples and zinc oxide's significant toxicity and titanium dioxide bioenergetics effect on FFA patient derived fibroblasts may suggest a possible causative link between FFA and nanoparticle-based sunscreen ingredients, however, this warrants further study.

Although the results presented in this study are not conclusive the consistent results using different investigations are supportive of further experimental studies to elucidate the exact mechanism by which sunscreen actives could be contributing to the development and progression of FFA.

REFERENCES

1. Buffoli B, Rinaldi F, Labanca M, Sorbellini E, Trink A, Guanziroli E, et al. The human hair: from anatomy to physiology. Int J Dermatol. 2014;53(3):331-41.
2. Wolff H, Fischer TW, Blume-Peytavi U. The Diagnosis and Treatment of Hair and Scalp Diseases. Dtsch Arztebl Int. 2016;113(21):377-86.
3. Pierard-Franchimont C, Pierard GE. Alterations in hair follicle dynamics in women. Biomed Res Int. 2013;2013:957432.
4. Alonso L, Fuchs E. The hair cycle. J Cell Sci. 2006;119(Pt 3):391-3.
5. Tanus A, Oliveira CCC, Villarreal DJV, Sanchez FAV, Dias MFRG. Black women's hair: the main scalp dermatoses and aesthetic practices in women of African ethnicity. Anais brasileiros de dermatologia. 2015;90(4):450-65.
6. Anzai A, Donati A, Valente NY, Romiti R, Tosti A. Isolated eyebrow loss in frontal fibrosing alopecia: relevance of early diagnosis and treatment. Br J Dermatol. 2016;175(5):1099-101.
7. Lee Y, Kim YD, Pi Lq, Lee SY, Hong H, Lee WS. Comparison of hair shaft damage after chemical treatment in A sian, W hite E uropean, and A frican hair. International journal of dermatology. 2014;53(9):1103-10.
8. Sellheyer K, Bergfeld WF. Histopathologic evaluation of alopecias. Am J Dermatopathol. 2006;28(3):236-59.
9. Sundberg JP, Hordinsky MK, Bergfeld W, Lenzy YM, McMichael AJ, Christiano AM, et al. Cicatricial Alopecia Research Foundation meeting, May 2016: Progress towards the diagnosis, treatment and cure of primary cicatricial alopecias. Exp Dermatol. 2018;27(3):302-10.
10. Vujovic A, Del Marmol V. The female pattern hair loss: review of etiopathogenesis and diagnosis. Biomed Res Int. 2014;2014:767628.
11. Moure ER, Romiti R, Machado MC, Valente NY. Primary cicatricial alopecias: a review of histopathologic findings in 38 patients from a clinical university hospital in Sao Paulo, Brazil. Clinics (Sao Paulo). 2008;63(6):747-52.
12. Filbrandt R, Rufaut N, Jones L, Sinclair R. Primary cicatricial alopecia: diagnosis and treatment. CMAJ. 2013;185(18):1579-85.
13. Zaouak A, Ghorbel HH, Badri T, Koubaa W, Fenniche S. Frontotemporal hairline recession in a postmenopausal woman. Dermatol Pract Concept. 2015;5(2):129-31.

14. Moreno-Arrones OM, Saceda-Corralo D, Fonda-Pascual P, Rodrigues-Barata AR, Buendia-Castano D, Alegre-Sanchez A, et al. Frontal fibrosing alopecia: clinical and prognostic classification. J Eur Acad Dermatol Venereol. 2017;31(10):1739-45.
15. Tziotzios C, Stefanato CM, Fenton DA, Simpson MA, McGrath JA. Frontal fibrosing alopecia: reflections and hypotheses on aetiology and pathogenesis. Exp Dermatol. 2016;25(11):847-52.
16. Donati A. Frontal fibrosing alopecia and sunscreens: cause or consequence? Br J Dermatol. 2016;175(4):675-6.
17. Aldoori N, Dobson K, Holden CR, McDonagh AJ, Harries M, Messenger AG. Frontal fibrosing alopecia: possible association with leave-on facial skin care products and sunscreens; a questionnaire study. Br J Dermatol. 2016;175(4):762-7.
18. Pastrana H, Avila A, Tsai CSJ. Nanomaterials in Cosmetic Products: the Challenges with regard to Current Legal Frameworks and Consumer Exposure. NanoEthics. 2018;12(2):123-37.
19. Antje Grobe ORaAJDG. Risk Governance of Nanotechnology Applications in Food and Cosmetics. Geneva, Switzerland: international risk governance council; 2008.
20. Ajazzuddin M, Jeswani G, Jha A. Nanocosmetics: Past, Present and Future Trends. Recent Patents on Nanomedicine. 2015;5(1):3-11.
21. Nohynek GJ, Dufour EK. Nano-sized cosmetic formulations or solid nanoparticles in sunscreens: a risk to human health? Arch Toxicol. 2012;86(7):1063-75.
22. Brunet-Possenti F, Deschamps L, Colboc H, Somogyi A, Medjoubi K, Bazin D, et al. Detection of titanium nanoparticles in the hair shafts of a patient with frontal fibrosing alopecia. J Eur Acad Dermatol Venereol. 2018;32(12):e442-e3.
23. Thompson CT, Chen ZQ, Kolivras A, Tosti A. Identification of titanium dioxide on the hair shaft of patients with and without frontal fibrosing alopecia: A pilot study of 20 patients. Br J Dermatol. 2019.
24. Diffey BL, Brown MW. The ideal spectral profile of topical sunscreens. Photochem Photobiol. 2012;88(3):744-7.
25. Mommaas AM, van Praag MC, Bouwes Bavinck JN, Out-Luiting C, Vermeer BJ, Claas FH. Analysis of the protective effect of topical sunscreens on the UVB-radiation-induced suppression of the mixed-lymphocyte reaction. J Invest Dermatol. 1990;95(3):313-6.
26. Gonzalez S, Fernandez-Lorente M, Gilaberte-Calzada Y. The latest on skin photoprotection. Clin Dermatol. 2008;26(6):614-26.

27. Cario-Andre M, Briganti S, Picardo M, Nikaido O, Gall Y, Ginestar J, et al. Epidermal reconstructs: a new tool to study topical and systemic photoprotective molecules. Journal of photochemistry and photobiology B, Biology. 2002;68(2-3):79-87.

28. Jansen R, Osterwalder U, Wang SQ, Burnett M, Lim HW. Photoprotection: part II. Sunscreen: development, efficacy, and controversies. J Am Acad Dermatol. 2013;69(6):867 e1-14; quiz 81-2.

29. Hanigan D, Truong L, Schoepf J, Nosaka T, Mulchandani A, Tanguay RL, et al. Trade-offs in ecosystem impacts from nanomaterial versus organic chemical ultraviolet filters in sunscreens. Water Res. 2018;139:281-90.

30. De Matteis V. Exposure to Inorganic Nanoparticles: Routes of Entry, Immune Response, Biodistribution and In Vitro/In Vivo Toxicity Evaluation. Toxics. 2017;5(4).

31. Khan M, Naqvi AH, Ahmad M. Comparative study of the cytotoxic and genotoxic potentials of zinc oxide and titanium dioxide nanoparticles. Toxicology reports. 2015;2:765-74.

32. Larese Filon F, Mauro M, Adami G, Bovenzi M, Crosera M. Nanoparticles skin absorption: New aspects for a safety profile evaluation. Regulatory toxicology and pharmacology : RTP. 2015;72(2):310-22.

33. De Matteis V, Malvindi MA, Galeone A, Brunetti V, De Luca E, Kote S, et al. Negligible particle-specific toxicity mechanism of silver nanoparticles: the role of Ag+ ion release in the cytosol. Nanomedicine : nanotechnology, biology, and medicine. 2015;11(3):731-9.

34. Maslin DL. Do suncreens protect us? International journal of dermatology. 2014;53(11):1319-23.

35. Gaspar NK. DHEA and frontal fibrosing alopecia: molecular and physiopathological mechanisms. An Bras Dermatol. 2016;91(6):776-80.

36. Ma SA, Imadojemu S, Beer K, Seykora JT. Inflammatory features of frontal fibrosing alopecia. J Cutan Pathol. 2017;44(8):672-6.

37. Callender VD, Reid SD, Obayan O, McClellan L, Sperling L. Diagnostic Clues to Frontal Fibrosing Alopecia in Patients of African Descent. J Clin Aesthet Dermatol. 2016;9(4):45-51.

38. Vano-Galvan S, Molina-Ruiz AM, Serrano-Falcon C, Arias-Santiago S, Rodrigues-Barata AR, Garnacho-Saucedo G, et al. Frontal fibrosing alopecia: a multicenter review of 355 patients. J Am Acad Dermatol. 2014;70(4):670-8.

39. Dlova NC, Jordaan HF, Skenjane A, Khoza N, Tosti A. Frontal fibrosing alopecia: a clinical review of 20 black patients from South Africa. Br J Dermatol. 2013;169(4):939-41.

40. Dlova NC, Goh CL. Frontal fibrosing alopecia in an African man. Int J Dermatol. 2015;54(1):81-3.

41. Dlova NC, Dadzie OE. Frontal Fibrosing Alopecia Severity Index (FFASI): a call for a more inclusive and globally relevant severity index for frontal fibrosing alopecia. Br J Dermatol. 2017;177(3):883-4.

42. Esteban-Lucia L, Molina-Ruiz AM, Requena L. Update on Frontal Fibrosing Alopecia. Actas Dermosifiliogr. 2017;108(4):293-304.

43. Tziotzios C, Fenton DA, Stefanato CM, McGrath JA. Familial frontal fibrosing alopecia. J Am Acad Dermatol. 2015;73(1):e37.

44. Iorizzo M, Tosti A. Frontal Fibrosing Alopecia: An Update on Pathogenesis, Diagnosis, and Treatment. Am J Clin Dermatol. 2019;20(3):379-90.

45. Miteva M, Castillo D, Sabiq S. Adipose Infiltration of the Dermis, Involving the Arrector Pili Muscle, and Dermal Displacement of Eccrine Sweat Coils: New Histologic Observations in Frontal Fibrosing Alopecia. Am J Dermatopathol. 2019.

46. Harries MJ, Meyer KC, Paus R. Hair loss as a result of cutaneous autoimmunity: frontiers in the immunopathogenesis of primary cicatricial alopecia. Autoimmun Rev. 2009;8(6):478-83.

47. Bernard BA. <Advances in Understanding Hair Growth.pdf>. 2016.

48. K.C. Meyer JEK, * H.V. Dinh, M.J. Harries,*§ K. Reithmayer,* W. Meyer,** R. Sinclair and R. Paus*–. <C.-2008-Br._J._Dermatol..pdf>. 2008.

49. Harries MJ, Jimenez F, Izeta A, Hardman J, Panicker SP, Poblet E, et al. Lichen Planopilaris and Frontal Fibrosing Alopecia as Model Epithelial Stem Cell Diseases. Trends Mol Med. 2018;24(5):435-48.

50. Ranasinghe GC, Piliang MP, Bergfeld WF. Prevalence of hormonal and endocrine dysfunction in patients with lichen planopilaris (LPP): A retrospective data analysis of 168 patients. J Am Acad Dermatol. 2017;76(2):314-20.

51. To D, Beecker J. Frontal Fibrosing Alopecia: Update and Review of Challenges and Successes. J Cutan Med Surg. 2018;22(2):182-9.

52. Tziotzios C, Stefanato CM, Fenton DA, Simpson MA, McGrath JA. Frontal fibrosing alopecia: reflections and hypotheses on aetiology and pathogenesis. 2016. In:

Experimental dermatology [Internet]. [847-52]. Available from: https://onlinelibrary.wiley.com/doi/pdf/10.1111/exd.13071.

53. Lu PJ, Huang SC, Chen YP, Chiueh LC, Shih DY. Analysis of titanium dioxide and zinc oxide nanoparticles in cosmetics. J Food Drug Anal. 2015;23(3):587-94.

54. Burnett ME, Wang SQ. Current sunscreen controversies: a critical review. Photodermatol Photoimmunol Photomed. 2011;27(2):58-67.

55. Makumire S, Chakravadhanula VS, Köllisch G, Redel E, Shonhai A. Immunomodulatory activity of zinc peroxide (ZnO 2) and titanium dioxide (TiO 2) nanoparticles and their effects on DNA and protein integrity. Toxicology letters. 2014;227(1):56-64.

56. Krause M, Klit A, Blomberg Jensen M, Søeborg T, Frederiksen H, Schlumpf M, et al. Sunscreens: are they beneficial for health? An overview of endocrine disrupting properties of UV-filters. International journal of andrology. 2012;35(3):424-36.

57. Lozano-Fernandez T, Ballester-Antxordoki L, Perez-Temprano N, Rojas E, Sanz D, Iglesias-Gaspar M, et al. Potential impact of metal oxide nanoparticles on the immune system: The role of integrins, L-selectin and the chemokine receptor CXCR4. Nanomedicine : nanotechnology, biology, and medicine. 2014;10(6):1301-10.

58. Jallad KN. Chemical characterization of sunscreens composition and its related potential adverse health effects. J Cosmet Dermatol. 2017;16(3):353-7.

59. Lim HW, Arellano-Mendoza MI, Stengel F. Current challenges in photoprotection. J Am Acad Dermatol. 2017;76(3S1):S91-S9.

60. Couteau C, Couteau O, Alami-El Boury S, Coiffard L. Sunscreen products: What do they protect us from? International journal of pharmaceutics. 2011;415(1-2):181-4.

61. Sambandan DR, Ratner D. Sunscreens: an overview and update. J Am Acad Dermatol. 2011;64(4):748-58.

62. Litaiem N, Idoudi SI. Frontal Fibrosing Alopecia. StatPearls. Treasure Island (FL): StatPearls Publishing

StatPearls Publishing LLC.; 2019.

63. Muireann Roche MYW, D. K. B. Armstrong. <FFA occurrence in male and demale siblings.pdf>. JAM ACAD DERMATOL. 2008.

64. Porrino-Bustamante ML, Lopez-Nevot MA, Aneiros-Fernandez J, Garcia-Lora E, Fernandez-Pugnaire MA, Arias-Santiago S. Familial frontal fibrosing alopecia: A cross-sectional study of 20 cases from nine families. Australas J Dermatol. 2019;60(2):e113-e8.

65. Chan DV, Kartono F, Ziegler R, Abdulwahab N, DiPaola N, Flynn J, et al. Absence of HLA-DR1 positivity in 2 familial cases of frontal fibrosing alopecia. J Am Acad Dermatol. 2014;71(5):e208-10.

66. Rivas MM, Antolin SC, Sambucety PS, Gonzalez ES, Ruiz de Morales JM, Prieto MA. Frontal fibrosing alopecia and lichen planopilaris in HLA-identical mother and daughter. Indian J Dermatol Venereol Leprol. 2015;81(2):162-5.

67. Porrino-Bustamante ML, Lopez-Nevot MA, Aneiros-Fernandez J, Casado-Ruiz J, Garcia-Linares S, Pedrinacci-Rodriguez S, et al. Study of Human Leukocyte Antigen (HLA) in 13 cases of familial frontal fibrosing alopecia: CYP21A2 gene p.V281L mutation from congenital adrenal hyperplasia linked to HLA class I haplotype HLA-A*33:01; B*14:02; C*08:02 as a genetic marker. Australas J Dermatol. 2019.

68. Meyer D, VR CA, Bitarello BD, DY CB, Nunes K. A genomic perspective on HLA evolution. Immunogenetics. 2018;70(1):5-27.

69. Wang M, Claesson MH. Classification of human leukocyte antigen (HLA) supertypes. Methods in molecular biology (Clifton, NJ). 2014;1184:309-17.

70. Trowsdale J. The MHC, disease and selection. Immunol Lett. 2011;137(1-2):1-8.

71. Danchin E, Vitiello V, Vienne A, Richard O, Gouret P, McDermott MF, et al. The major histocompatibility complex origin. Immunological reviews. 2004;198:216-32.

72. Tziotzios C, Petridis C, Dand N, Ainali C, Saklatvala JR, Pullabhatla V, et al. Genome-wide association study in frontal fibrosing alopecia identifies four susceptibility loci including HLA-B*07:02. Nature communications. 2019;10(1):1150.

73. Fertig R, Tosti A. Frontal fibrosing alopecia treatment options. Intractable Rare Dis Res. 2016;5(4):314-5.

74. Perez-Rodriguez IM, Garcia-Melendez ME, Eichelmann K, Vazquez-Martinez O, Ocampo-Candiani J. Hyperpigmentation following Treatment of Frontal Fibrosing Alopecia. Case Rep Dermatol. 2013;5(3):357-62.

75. Fertig R, Aleid NM, Antonella T. Therapeutic options in frontal fibrosing alopecia. Expert Opinion on Orphan Drugs. 2016;4(5):461-8.

76. Donovan JC. Finasteride-mediated hair regrowth and reversal of atrophy in a patient with frontal fibrosing alopecia. JAAD Case Rep. 2015;1(6):353-5.

77. Fenton CTCMSDA, McGrath MASJA. Frontal fibrosing alopecia: reflections and hypotheses on

aetiology and pathogenesis [REVIEW]2016.

78. Gunasegaran J. Textbook of Histology and Practical guide: Elsevier Health Sciences; 2014.

79. Girão AV, Caputo G, Ferro MC. Application of Scanning Electron Microscopy–Energy Dispersive X-Ray Spectroscopy (SEM-EDS). Comprehensive Analytical Chemistry. 75: Elsevier; 2017. p. 153-68.

80. Girao AV, Caputo G, Ferro MC. Application of Scanning Electron Microscopy-Energy Dispersive X-ray Spectroscopy (SEM-EDS)2017.

81. Newbury DE, Ritchie NW. Is Scanning Electron Microscopy/Energy Dispersive X-ray Spectrometry (SEM/EDS) Quantitative? Scanning. 2013;35(3):141-68.

82. Hollerith C, Wernicke D, Buhler M. Energy dispersive X-ray spectroscopy with microcalorimeters. Nuclear Instruments & Methods in Physics Research Section a-Accelerators Spectrometers Detectors and Associated Equipment. 2004;520(1-3):606-9.

83. Ngo PD. Energy dispersive spectroscopy. Failure Analysis of Integrated Circuits: Springer; 1999. p. 205-15.

84. Hafner B. Energy Dispersive Spectroscopy on the SEM:

A Primer. Characterization Facility, University of Minnesota—Twin Cities.

85. Newbury DE, Ritchie NWM. Elemental mapping of microstructures by scanning electron microscopy-energy dispersive X-ray spectrometry (SEM-EDS): extraordinary advances with the silicon drift detector (SDD). Journal of Analytical Atomic Spectrometry. 2013;28(7):973-88.

86. Movasaghi Z, Rehman S, Rehman IU. Fourier transform infrared (FTIR) spectroscopy of biological tissues. Applied Spectroscopy Reviews. 2008;43(2):134-79.

87. Kazarian SG, Chan KL. ATR-FTIR spectroscopic imaging: recent advances and applications to biological systems. Analyst. 2013;138(7):1940-51.

88. Setnička V. <FTIR Reflection Techniques.pdf>.

89. Stuart B. <FTIR ANALYSIS GUIDELINES.pdf>.

90. Spectroscopy I. <ir_presentation.pdf>.

91. Gorzsas A, Stenlund H, Persson P, Trygg J, Sundberg B. Cell-specific chemotyping and multivariate imaging by combined FT-IR microspectroscopy and orthogonal projections to latent structures (OPLS) analysis reveals the chemical landscape of secondary xylem. Plant J. 2011;66(5):903-14.

92. Trygg J, Holmes E, Lundstedt T. Chemometrics in metabonomics. Journal of proteome research. 2007;6(2):469-79.

93. Mori Y, Okastu Y, Tsujimoto Y. Titanium dioxide nanoparticles produced in water-in-oil emulsion. Journal of Nanoparticle Research. 2001;3(2-3):219-25.
94. Gamer AO, Leibold E, van Ravenzwaay B. The in vitro absorption of microfine zinc oxide and titanium dioxide through porcine skin. Toxicology in Vitro. 2006;20(3):301-7.
95. PubChem. Sodium Lauryl Sulfate 2019 [Available from: National Center for Biotechnology Information. PubChem Compound Database; CID=3423265, https://pubchem.ncbi.nlm.nih.gov/compound/3423265 (accessed Feb. 11, 2019).
96. Dojindo Molecular Technologies I. http://www.dojindo.com/store/p/456-Cell-Counting-Kit-8.html [
97. MERCK. Cell Counting Kit - 8 2018 [Available from: https://www.sigmaaldrich.com/catalog/product/sigma/96992?lang=en&region=ZA&gclid=EAIaIQobChMInue55_bK2QIVCr7tCh2_dg-FEAAYAiAAEgLou_D_BwE.
98. Aslantürk ÖS. In Vitro Cytotoxicity and Cell Viability Assays: Principles, Advantages, and Disadvantages. 2018.
99. Menyhart O, Harami-Papp H, Sukumar S, Schafer R, Magnani L, de Barrios O, et al. Guidelines for the selection of functional assays to evaluate the hallmarks of cancer. Biochim Biophys Acta. 2016;1866(2):300-19.
100. Bioarray C. Comparison of Different Methods to Measure Cell Viability 2019 [Available from: https://www.creative-bioarray.com/support/comparison-of-different-methods-to-measure-cell-viability.htm.
101. Terry L, Richard A, Andrew L, Helene A, Tracy J, Lisa M, et al. Cell viability assays. Assay Guidance Manual. 2015;29:27-31.
102. Leung DT, Chu S. Measurement of Oxidative Stress: Mitochondrial Function Using the Seahorse System. Preeclampsia: Springer; 2018. p. 285-93.
103. Contin LA, de Almeida Leda YL, Caldeira Nassif K, Suarez Restrepo MV. Patchy Frontal Fibrosing Alopecia: Description of an Incomplete Clinical Presentation. Skin Appendage Disord. 2017;3(4):190-2.
104. Murad A, Bergfeld W. 5-alpha-reductase inhibitor treatment for frontal fibrosing alopecia: an evidence-based treatment update. J Eur Acad Dermatol Venereol. 2018.
105. Strazzulla LC, Avila L, Li X, Lo Sicco K, Shapiro J. Prognosis, treatment, and disease outcomes in frontal fibrosing alopecia: A retrospective review of 92 cases. J Am Acad Dermatol. 2018;78(1):203-5.

106. Brandi N, Starace M, Alessandrini A, Bruni F, Piraccini BM. The doll hairline: A clue for the diagnosis of frontal fibrosing alopecia. J Am Acad Dermatol. 2017;77(5):e127-e8.

107. Katoulis AC, Christodoulou C, Liakou AI, Kouris A, Korkoliakou P, Kaloudi E, et al. Quality of life and psychosocial impact of scarring and non-scarring alopecia in women. Journal der Deutschen Dermatologischen Gesellschaft = Journal of the German Society of Dermatology : JDDG. 2015;13(2):137-42.

108. Hunt N, McHale S. The psychological impact of alopecia. BMJ. 2005;331(7522):951-3.

109. Moreno-Arrones OM, Saceda-Corralo D, Rodrigues-Barata AR, Castellanos-Gonzalez M, Pugnaire MA, Grimalt R, et al. Risk factors associated with frontal fibrosing alopecia: a multicentre case-control study. Clin Exp Dermatol. 2018.

110. Callander J, Frost J, Stone N. Ultraviolet filters in hair-care products: a possible link with frontal fibrosing alopecia and lichen planopilaris. Clin Exp Dermatol. 2018;43(1):69-70.

111. Brunet-Possenti F, Deschamps L, Colboc H, Somogyi A, Medjoubi K, Bazin D, et al. Detection of titanium nanoparticles in the hair shafts of a patient with frontal fibrosing alopecia. J Eur Acad Dermatol Venereol. 2018.

112. Das A, Biswas A, Guha Mazumder DN. Association between skin lesion and arsenic concentration in hair by mixed bivariate model in chronic arsenic exposure. Environmental geochemistry and health. 2018.

113. McMillan TM, Jacobson RR, Gross M. Neuropsychology of thallium poisoning. Journal of neurology, neurosurgery, and psychiatry. 1997;63(2):247-50.

114. Yang G, Li C, Long Y, Sheng L. Hair Loss: Evidence to Thallium Poisoning. Case reports in emergency medicine. 2018;2018:1313096.

115. Yu V, Juhász M, Chiang A, Atanaskova Mesinkovska N. Alopecia and Associated Toxic Agents: A Systematic Review. Skin Appendage Disorders. 2018;4(4):245-60.

116. Bocca B, Pino A, Alimonti A, Forte G. Toxic metals contained in cosmetics: a status report. Regulatory toxicology and pharmacology : RTP. 2014;68(3):447-67.

117. Borowska S, Brzoska MM. Metals in cosmetics: implications for human health. Journal of applied toxicology : JAT. 2015;35(6):551-72.

118. Iwegbue CMA, Emakunu OS, Obi G, Nwajei GE, Martincigh BS. Evaluation of human exposure to metals from some commonly used hair care products in Nigeria. Toxicology reports. 2016;3:796-803.

119. LENNTECH. 2019 [Available from: https://www.lenntech.com/periodic/elements/as.htm.

120. Dicle O, Celik-Ozenci C, Sahin P, Pfannes EKB, Vogt A, Altinok BN, et al. Differential expression of mTOR signaling pathway proteins in lichen planopilaris and frontal fibrosing alopecia. Acta histochemica. 2018.

121. Donati A, Gupta AK, Jacob C, Cavelier-Balloy B, Reygagne P. The Use of Direct Immunofluorescence in Frontal Fibrosing Alopecia. Skin Appendage Disord. 2017;3(3):125-8.

122. Galvez-Canseco A, Sperling L. Lichen planopilaris and frontal fibrosing alopecia cannot be differentiated by histopathology. J Cutan Pathol. 2018;45(5):313-7.

123. Geology.com. Strontium Titanate 2019 [Available from: https://geology.com/gemstones/strontium-titanate/.

124. George CN, Thomas JK, Jose R, Kumar HP, Suresh MK, Kumar VR, et al. Synthesis and characterization of nanocrystalline strontium titanate through a modified combustion method and its sintering and dielectric properties. Journal of Alloys and Compounds. 2009;486(1-2):711-5.

125. Makarova M, Dejneka A, Franc J, Drahokoupil J, Jastrabik L, Trepakov V. Soft chemistry preparation methods and properties of strontium titanate nanoparticles. Optical Materials. 2010;32(8):803-6.

126. Palm MD, O'Donoghue MN. Update on photoprotection. Dermatol Ther. 2007;20(5):360-76.

127. Subramaniam VD, Prasad SV, Banerjee A, Gopinath M, Murugesan R, Marotta F, et al. Health hazards of nanoparticles: understanding the toxicity mechanism of nanosized ZnO in cosmetic products. Drug and chemical toxicology. 2018:1-10.

128. Titma T, Shimmo R, Siigur J, Kahru A. Toxicity of antimony, copper, cobalt, manganese, titanium and zinc oxide nanoparticles for the alveolar and intestinal epithelial barrier cells in vitro. Cytotechnology. 2016;68(6):2363-77.

129. Schneider T, Westermann M, Glei M. In vitro uptake and toxicity studies of metal nanoparticles and metal oxide nanoparticles in human HT29 cells. Arch Toxicol. 2017;91(11):3517-27.

130. Ao J, Yuan T, Gao L, Yu X, Zhao X, Tian Y, et al. Organic UV filters exposure induces the production of inflammatory cytokines in human macrophages. The Science of the total environment. 2018;635:926-35.

131. Barr L, Alamer M, Darbre PD. Measurement of concentrations of four chemical ultraviolet filters in human breast tissue at serial locations across the breast. Journal of applied toxicology : JAT. 2018;38(8):1112-20.
132. Frikeche J, Couteau C, Roussakis C, Coiffard LJ. Research on the immunosuppressive activity of ingredients contained in sunscreens. Arch Dermatol Res. 2015;307(3):211-8.
133. Gulston M, Knowland J. Illumination of human keratinocytes in the presence of the sunscreen ingredient Padimate-O and through an SPF-15 sunscreen reduces direct photodamage to DNA but increases strand breaks. Mutation research. 1999;444(1):49-60.
134. Mendoza J, Sebastian A, Allan E, Allan D, Mandal P, Alonso-Rasgado T, et al. Differential cytotoxic response in keloid fibroblasts exposed to photodynamic therapy is dependent on photosensitiser precursor, fluence and location of fibroblasts within the lesion. Archives of Dermatological Research. 2012;304(7):549-62.
135. van Meerloo J, Kaspers GJ, Cloos J. Cell sensitivity assays: the MTT assay. Cancer cell culture: Springer; 2011. p. 237-45.
136. van Tonder A, Joubert AM, Cromarty AD. Limitations of the 3-(4,5-dimethylthiazol-2-yl)-2,5-diphenyl-2H-tetrazolium bromide (MTT) assay when compared to three commonly used cell enumeration assays. BMC Res Notes. 2015;8:47.
137. Scudiero DA, Shoemaker RH, Paull KD, Monks A, Tierney S, Nofziger TH, et al. Evaluation of a soluble tetrazolium/formazan assay for cell growth and drug sensitivity in culture using human and other tumor cell lines. Cancer research. 1988;48(17):4827-33.
138. Van Tonder A, Joubert AM, Cromarty AD. Limitations of the 3-(4, 5-dimethylthiazol-2-yl)-2, 5-diphenyl-2H-tetrazolium bromide (MTT) assay when compared to three commonly used cell enumeration assays. BMC research notes. 2015;8(1):47.
139. Kroll A, Pillukat MH, Hahn D, Schnekenburger J. Current in vitro methods in nanoparticle risk assessment: limitations and challenges. Eur J Pharm Biopharm. 2009;72(2):370-7.
140. Aldrich S. https://www.sigmaaldrich.com/content/dam/sigma-aldrich/docs/Roche/Bulletin/1/11644793001bul.pdf. 2016.
141. Smith SM, Wunder MB, Norris DA, Shellman YG. A simple protocol for using a LDH-based cytotoxicity assay to assess the effects of death and growth inhibition at the same time. PLoS One. 2011;6(11):e26908.
142. Kroll A, Pillukat MH, Hahn D, Schnekenburger J. Interference of engineered nanoparticles with in vitro toxicity assays. Arch Toxicol. 2012;86(7):1123-36.

143. Holder AL, Goth-Goldstein R, Lucas D, Koshland CP. Particle-induced artifacts in the MTT and LDH viability assays. Chem Res Toxicol. 2012;25(9):1885-92.

APPENDICES

Appendix 1: SEM/EDS detected elements from the FFPE scalp sections

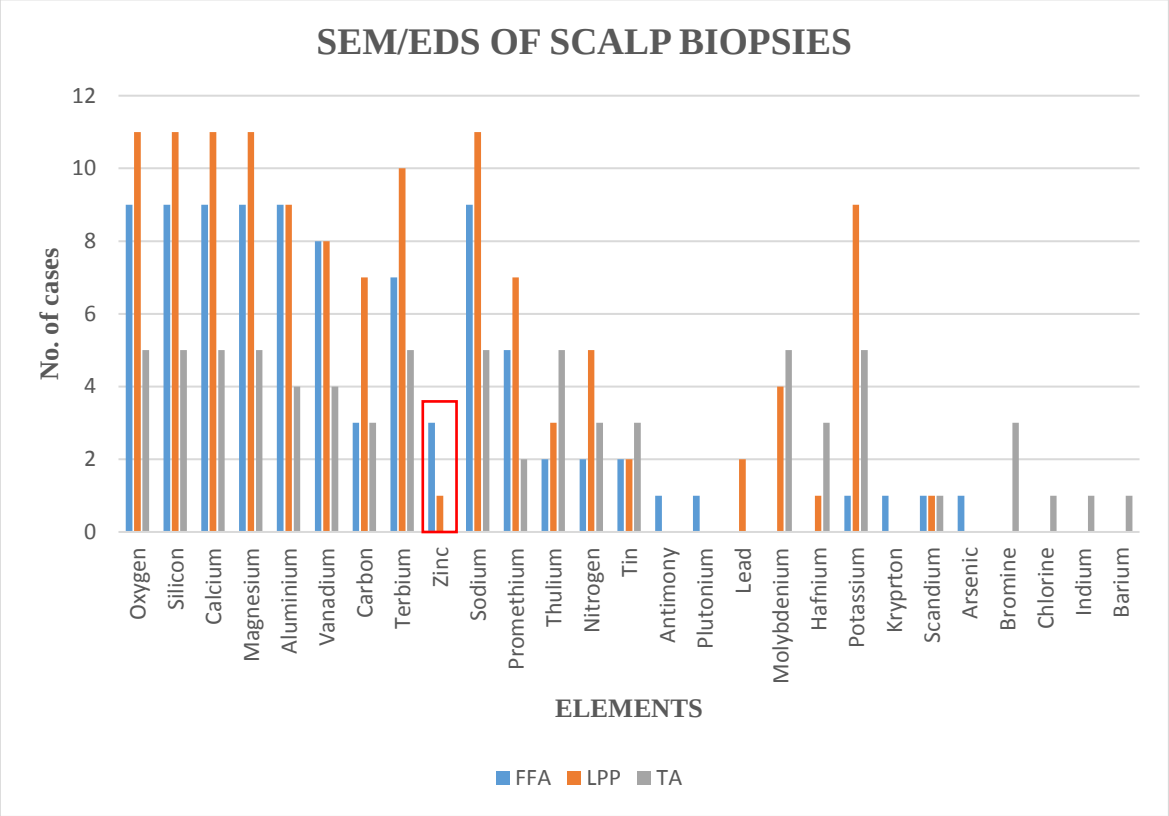

Figure 25 All element traces detected on the FFPE sections of FFA, LPP and TA, which includes an element of interest (zinc).

Table 6 Tabulated overall elements detected on the 20 archival scalp tissue sections.

	FFA 01	FFA 02	FFA 03	FFA 04	FFA 05	FFA 06	FFA 07	FFA 08	FFA 09	LPP 01	LPP 02	LPP 03	LPP 04	LPP 05	LPP 06	LPP 07	LPP 08	LPP 09	LPP 10	LPP 11	TA 01	TA 02	TA 03	TA 04	TA 05
oxygen	X	X	X	X	X	X	X	X	X	X	X	X	X	X	X	X	X	X	X	X	X	X	X	X	X
silicon	X	X	X	X	X	X	X	X	X	X	X	X	X	X	X	X	X	X	X	X	X	X	X	X	X
calcium	X	X	X	X	X	X	X	X	X	X	X	X	X	X	X	X	X	X	X	X	X	X	X	X	X
magnesium	X	X	X	X	X	X	X	X	X	X	X	X	X	X	X	X	X	X	X	X	X	X	X	X	X
aluminium	X	X	X	X	X	X	X	X	X	X	X	X			X	X	X	X	X	X	X	X		X	X
vanadium		X	X	X	X	X	X	X	X	X		X		X	X	X	X	X	X		X	X	X	X	
carbon		X		X					X	X	X		X		X	X	X	X			X	X	X	X	X
terbium	X	X			X	X	X	X	X	X	X	X	X	X	X	X		X	X	X	X	X	X	X	X
zinc	X		X						X			X													
sodium	X	X	X	X	X	X	X	X	X	X	X	X	X	X	X	X	X	X	X	X	X	X	X	X	X
promethium	X	X	X	X			X				X	X	X	X	X		X			X	X	X			
thulium		X	X							X					X			X			X	X	X	X	X
nitrogen				X					X		X	X			X	X		X			X		X	X	X
tin	X						X				X									X		X	X	X	
antimony		X																							
plutonium		X																							
lead										X	X														
molybdenum										X			X			X	X				X	X	X	X	X
hafnium													X								X			X	X
Potassium			X							X	X	X	X		X	X	X	X		X	X	X		X	X
Krypton			X																				X		
Scandium				X									X											X	
Arsenic				X																					
Bromine																					X	X		X	
Chlorine																								X	X
Indium																								X	

Appendix 2: Principal Component Analysis of the FTIR-ATR spectra of three types of hair loss conditions

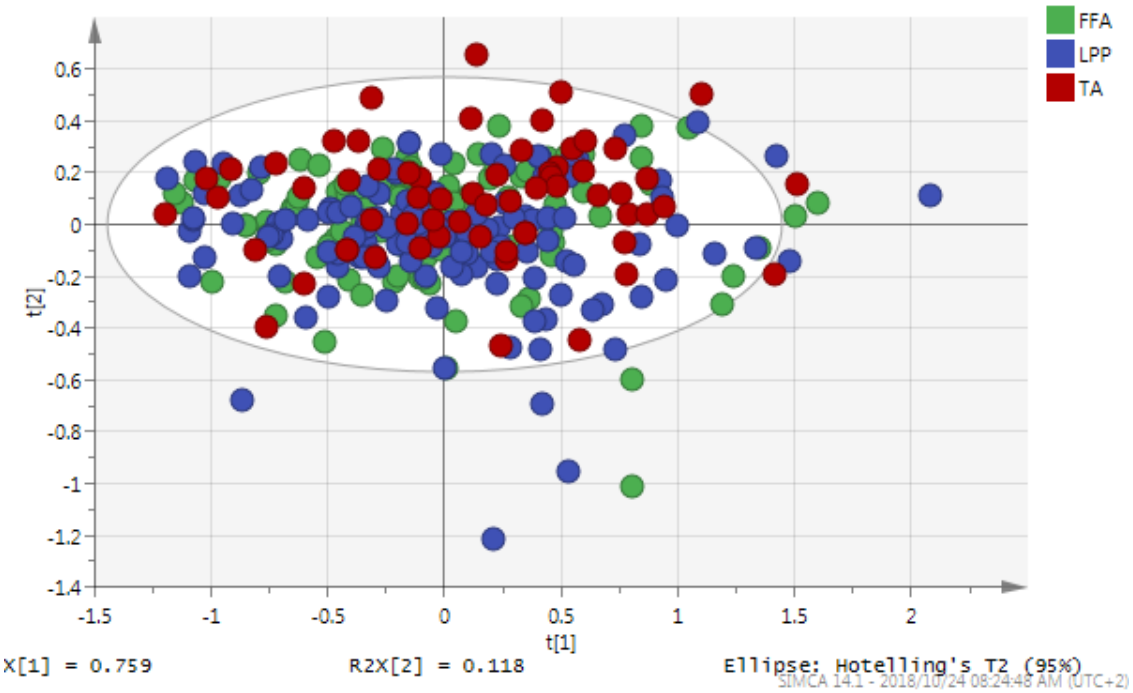

Figure 26 Principal Component Analysis of the FFA, LPP and TA FTIR-ATR spectra combined.

Table 7 FFA vs TA S-Plot Peaks and the compounds found within their range. Red (compounds responsible for most variation between the FFA and TA samples), black (compounds found on both the FFA and TA samples).

FFA vs TA	
Peaks (cm^{-1})	Compound
522-533	strontium titanate
599-596	potassium phosphate tribasic
670-1117	1,2-Dichloroethylene
1153-1174	Bromo(nitro)methane
1175-1206	5-Bromo-2-fluoro-m-xylene
1220	thionyl chloride
1276	Chloropentaaminecobalt(iii)Chloride
1300	hexachlorobenzene
1308	1-Chlorooctodecane
1356	sodium formate
1469-1472	calcium zirconate
1547-1549	Chloropentaaminecobalt(iii)Chloride
1581-1584	sodium formate
1608-1609	Molybdenum iodide anhydrous
1651	Indium sulfate
1655-1656	Sodium methyl carbonate
1662	3-Bromo-2-thiophenecarbaldehyde

Table 8 FFA vs LPP S-Plot Peaks and compounds found within their range. Red (compounds responsible for most variation between the FFA and LPP samples), black (compounds found on both the FFA and LPP samples). Lead chromate contributed to the biggest peak of separation between the two groups.

FFA vs LPP	
Peaks (cm^{-1})	Compound
47	Methiopropamine
60	3,4-Methylenedioxycathione
63	Cathione
69	URB-597
72	N-Ethylcathione HCl
79	Cathione HCl
88	URB-597
95-98	3-Flouromethcathione HCl
101-102	BZP diHCl
110	Dimethyltryptamine-Benzylpiperazine

112	α-PVT-HCl
130	Cathione
141	URB-597
151	3,4-Methylenedioxycathione
158-161	2-Methylmethcathione
171	Dimethyltryptamine
181-182	BZP diHCl
796-827	trans-1,2-Dichloroethylene
815-814	Lead chromate
1080-1082	Silica
1092	Magnesium-tert-butoxide
1103-1104	Neodymium fluoride
529	Strontium titanate
562-563	Potassium phosphate tribasic
1153	Tris(trimethylsilyloxy)ethylene
1160	ceric iodate
1117-1180	Algoflon 25 car
1198	trans-1,2-Dichloroethylene
1205	Deuterium
1206-1229	Thionyl chloride
1246	Acetone-d6
1305	Poly(hexafluoropropylene) oxide
1325-1326	Nitrocyclopentane
1363-1366	VM BP Naphtha
1434-1438	CX 1023
1489-1493	Strotium zirconate
1633	Potassium metaperiodate
1655-1656	Cobalt (iii) flouride
1661-1663	Formamide scandium sulfate
1665-1666	Potassium titanium dioxide oxalate dihydrate

Table 9 LPP vs TA S-Plot Peaks and the compounds found within their range. Red (compounds responsible for most variation between the LPP and TA samples), black (compounds found on both the LPP and TA samples).

LPP vs TA	
Peaks (cm^{-1})	Compound
1608-1610	Molybdenum iodide anhydrous
1619-1621	Sodium metaperiodate
518-543	Strontium titanate
557-568	Potassium phosphate tribasic
795-808	strontium molybdatee (vi)

812-816	Sodium metaperiodate
1151-1152	Poly (hexafluoropropylene oxide)
1156-1172	Poly (ethylene-methacrylate)
1187	Tin (ii) Trifluoromethanesulfonate
1225	Chlorobromomethane
1237	Methyl iodide
1253-1254	Trimethylchlorosilane
1271-1273	Lead bromide
1297-1300	Hezachlorobenzene
1356-1360	Sodium formate
1471-1474	Calcium zirconate
1502-1507	Chlorobromomethane
1548-1551	Chloropentaaminecobalt
1662	3-Bromo-2-thiophenecarbaldehyde
1659-1660	Magnesium oxalate

Appendix 3: Preparation of sunscreen actives

Preparation of 10% prop-glycol:

$$\%\ of\ substance = \frac{volume\ of\ solute}{volume\ of\ solution} \times 100$$

$$10\ \% = \frac{volume\ of\ solute}{50\ ml}$$

$$volume\ of\ solute = 10\ \% \times 50\ ml$$

$$volume\ of\ solute = 5\ ml$$

5 ml of prop-glycol + 45 ml of water were used to prepare 50 ml 10 % prop-glycol solution.

Preparation of 0.05 % SDS:

$$\%\ of\ substance = \frac{mass\ of\ constituent}{volume\ of\ solution} \times 100$$

$$0.05\ \% = \frac{mass\ of\ constituent}{50\ ml}$$

$$mass\ of\ constituent = 0.05\ \% \times 50\ ml$$

$$mass\ of\ constituent = 0.025\ g$$

0.025g of SDS was dissolved in 49.975 ml of water to prepare 50 ml 0.05 % SDS solution.

Titanium dioxide:

$$\%\ of\ substance = \frac{mass\ of\ constituent}{volume\ of\ solution} \times 100$$

$$5\ \% = \frac{mass\ of\ constituent}{20\ ml}$$

$mass\ of\ constituent = 5\ \% \times 20\ ml$

$mass\ of\ constituent = 1\ g$

1 g of TiO_2 was dissolved in 19 ml of 10% prop-glycol to prepare 20 ml 5 % TiO_2 solution.

Four more 2 ml serial dilutions of TiO_2 were made from the 5 % TiO_2 solution as follows:

4 % TiO_2 solution = 1.6 ml of 5 % TiO_2 solution + 0.4 ml of prop-glycol

3 % TiO_2 solution = 1.2 ml of 5 % TiO_2 solution + 0.8 ml of prop-glycol

2 % TiO_2 solution = 0.8 ml of 5 % TiO_2 solution + 1.2 ml of prop-glycol

1 % TiO_2 solution = 0.4 ml of 5 % TiO_2 solution + 1.6 ml of prop-glycol

Zinc oxide:

$$\%\ of\ substance = \frac{mass\ of\ constituent}{volume\ of\ solution} \times 100$$

$$5\ \% = \frac{mass\ of\ constituent}{20\ ml}$$

$mass\ of\ constituent = 5\ \% \times 20\ ml$

$mass\ of\ constituent = 1\ g$

1 g of ZnO was dissolved in 19 ml of 10% prop-glycol to prepare 20 ml 5 % ZnO solution.

Four more 2 ml serial dilutions of ZnO were made from the 5 % ZnO solution as follows:

4 % ZnO solution = 1.6 ml of 5 % ZnO solution + 0.4 ml of prop-glycol

3 % ZnO solution = 1.2 ml of 5 % ZnO solution + 0.8 ml of prop-glycol

2 % ZnO solution = 0.8 ml of 5 % ZnO solution + 1.2 ml of prop-glycol

1 % ZnO solution = 0.4 ml of 5 % ZnO solution + 1.6 ml of prop-glycol

Benzophenone-4:

$$\%\ of\ substance = \frac{mass\ of\ constituent}{volume\ of\ solution} \times 100$$

$$7.5\ \% = \frac{mass\ of\ constituent}{10\ ml}$$

$$mass\ of\ constituent = 7.5\ \% \times 10\ ml$$

$$mass\ of\ constituent = 0.75\ g$$

0.75 g of benzophenone-4 was dissolved in 9.25 ml of distilled water to prepare 10 ml 7.5 % benzophenone-4 solution.

Four more 2 ml serial dilutions of benzophenone-4 were made from the 7.5 % benzophenone-4 solution as follows:

5 % benzophenone-4 solution = 1.33 ml of 7.5 % benzophenone-4 solution + 0.67 ml of distilled water

3.5 % benzophenone-4 solution = 0.93 ml of 7.5 % benzophenone-4 solution + 1.07 ml of distilled water

2 % benzophenone-4 solution = 0.53 ml of 7.5 % benzophenone-4 solution + 1.47 ml of distilled water

1 % benzophenone-4 TiO_2 solution = 0.27 ml of 7.5 % benzophenone-4 solution + 1.73 ml of prop-glycol

Octinoxate:

$$\%\ of\ substance = \frac{volume\ of\ solute}{volume\ of\ solution} \times 100$$

$$7.5\ \% = \frac{volume\ of\ solute}{2\ ml}$$

$volume\ of\ solute = 7.5\ \% \times 2\ ml$

$volume\ of\ solute = 0.15\ ml$

∴ 0.15 ml of 100 % octinoxate + 1.85 ml of 0.05 % SDS were used to prepare 2 ml 7.5 % octinoxate.

Four more 2 ml serial dilutions of octinoxate were made using the same calculation method as above and the concentrations below were prepared:

5 % Octinoxate solution = 0.1 ml of 100 % octinoxate solution + 1.9 ml of 0.05 % SDS

3.5 % Octinoxate solution = 0.07 ml of 100 % octinoxate solution + 1.93 ml of 0.05 % SDS

2 % Octinoxate solution = 0.04 ml of 100 % octinoxate solution + 1.96 ml of 0.05 % SDS

1 % Octinoxate solution = 0.02 ml of 100 % octinoxate solution + 1.98 ml of 0.05 % SDS

Padimate O:

$$\%\ of\ substance = \frac{volume\ of\ solute}{volume\ of\ solution} \times 100$$

$$15\ \% = \frac{volume\ of\ solute}{2\ ml}$$

$volume\ of\ solute = 15\ \% \times 2\ ml$

$volume\ of\ solute = 0.30\ ml$

∴ 0.30 ml of 100 % padimate O + 1.75 ml of 0.05 % SDS were used to prepare 2 ml 15 % padimate O.

Four more 2 ml serial dilutions of padimate O were made using the same calculation method as above and the concentrations below were prepared:

10 % Padimate O solution = 0.2 ml of 100 % padimate O solution + 1.80 ml of 0.05 % SDS

5 % Padimate O solution = 0.1 ml of 100 % padimate O solution + 1.90 ml of 0.05 % SDS

2.5 % Padimate O solution = 0.05 ml of 100 % padimate O solution + 1.95 ml of 0.05 % SDS

1 % Padimate O solution = 0.02 ml of 100 % padimate O solution + 1.98 ml of 0.05 % SDS

Appendix 4: cytotoxic effect of sunscreen actives on cells (MTT assay) protocol

2.4.5. 3-(4,5-dimethylthiazol-2-yl)-2,5-diphenyltetrazolium bromide (MTT) assay

MMT it is a conventional well known colorimetric test used to determine the viability and cytotoxicity of cells, using the cells' mitochondrial activity (101). It is based on the mechanism of converting tetrazolium salt into purplish formazan dye crystals, using the mitochondria reductase, nicotinamide adenine dinucleotide (NADH) (135) . This mode of mechanism is outlined in (Figure *11*). The intensity of the dye colour is proportional to the viability of the cell's mitochondria (101). Although MTT has for many years has been considered a "gold standard" cytotoxicity assay, it has been of recent suggested unreliable, as due to its lack of reproducibility (101&136). Factors such as the inability of some cells to metabolise MTT which leads to the formation of the formazan crystals (137), are reasons for its questionable reliability. Moreover, the solubilizing of the formazan crystals step (138) required for this assay it is one of the limitations, as incomplete solubilization of the crystals may lead to inaccurate results. It is also reported that metal ions such as zinc ions interfere with the reduction rate of MTT (139)

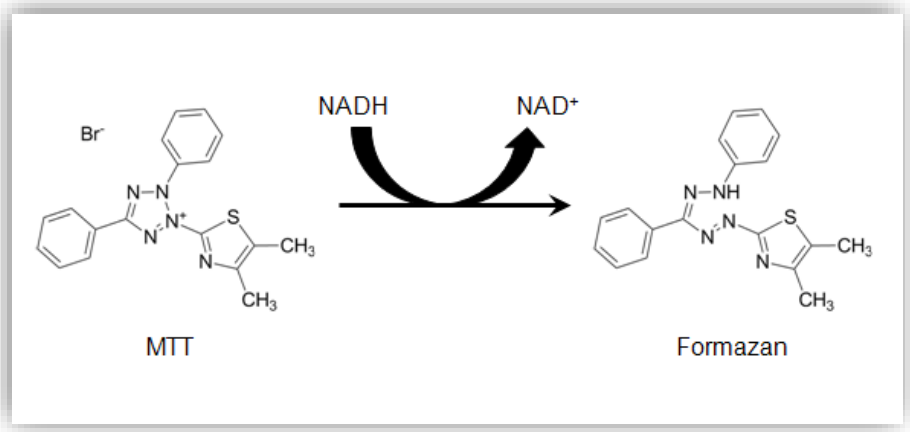

Figure 27 Mode of mechanism MTT uses to form its formazan dye (101)

We used MTT as part of our preliminary study and the assay resulted inconsistent and inaccurate results due to the aforementioned limitations of the assay. We could not rely on them; hence we could not include them in the study.

Appendix 5: cytotoxic effect of sunscreen actives on cells (LDH assay) protocol

2.4.6 Lactose dehydrogenase (LDH) cytotoxicity assay

LDH it is colorimetric assay for the quantification of cell death and cell lysis, based on the measurement of lactate dehydrogenase (LDH) activity released from the cytosol of damaged cells into the supernatant of the cell medium suspension (140). Plasma membrane damage during cell death leads to the release of LDH into the cell culture media. The mechanism of the assay is as outlined below (Figure *12*).

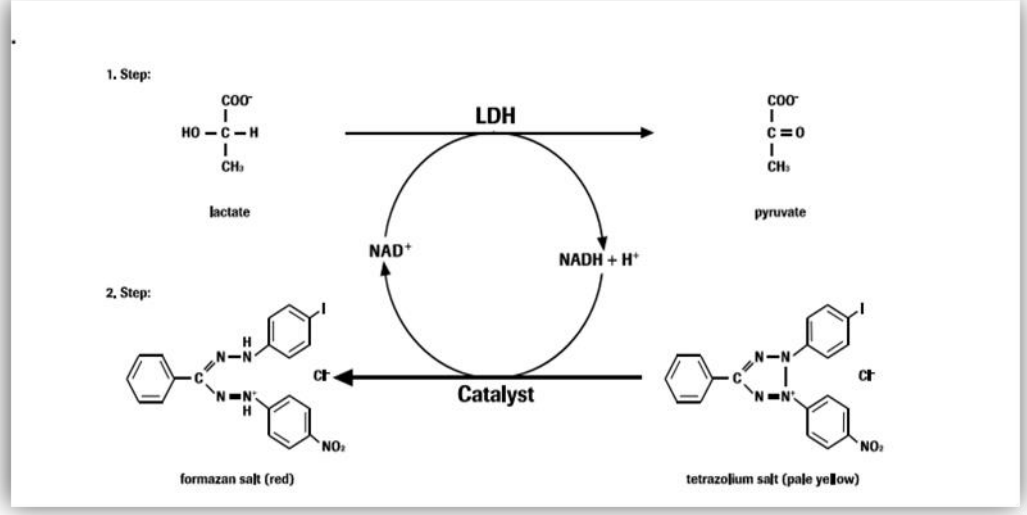

Figure 28 LDH assay mechanism (140)

As earlier described, cells were trypsinised and 2 x 10^4 cells per well were plated into 96 well plates, and they were left to adhere for 24 hrs in an incubator before treatment. After 24 hrs incubation, the culture medium was changed, and cells were treated with 100 µl of each active in varying concentrations (*Table 2*) in triplicate, according to the manufactures' instructions. The plate was left in the incubator for another 24 hrs before the LDH solution was added. After 24 hrs treatment, the microplate was centrifuged at 250 x g for 10 minutes, to allow detached cells to settle, so that we did not take them into the fresh plate and 100 µl

of the supernatant was transferred into a new microplate reader, followed by addition of 100 µl of the LDH solution. The microplate was then covered in a tin foil to protect reagent from light and left for 30 mins at room temperature before absorbance reading at 490 nm (140).

The results obtained were not reliable due to some limitations of LDH assay limitation. The sunscreen actives (especially inorganic actives) were interfering with the assays mechanisms to produce the formazan dye, which is required to measure the LDH released in the assay medium thus giving false negative results (Figure *28*). These limitations are well described in studies by (139&141&142), whereby it is mentioned that most nanoparticles due to their large surface area and high surface energy, they interact with assays' catalytic enzymes and fluorescent days, thereby introducing artefacts in the assay outcomes. Moreover, it is also reported that they may bind to LDH, thus reducing its detection in assays (143)

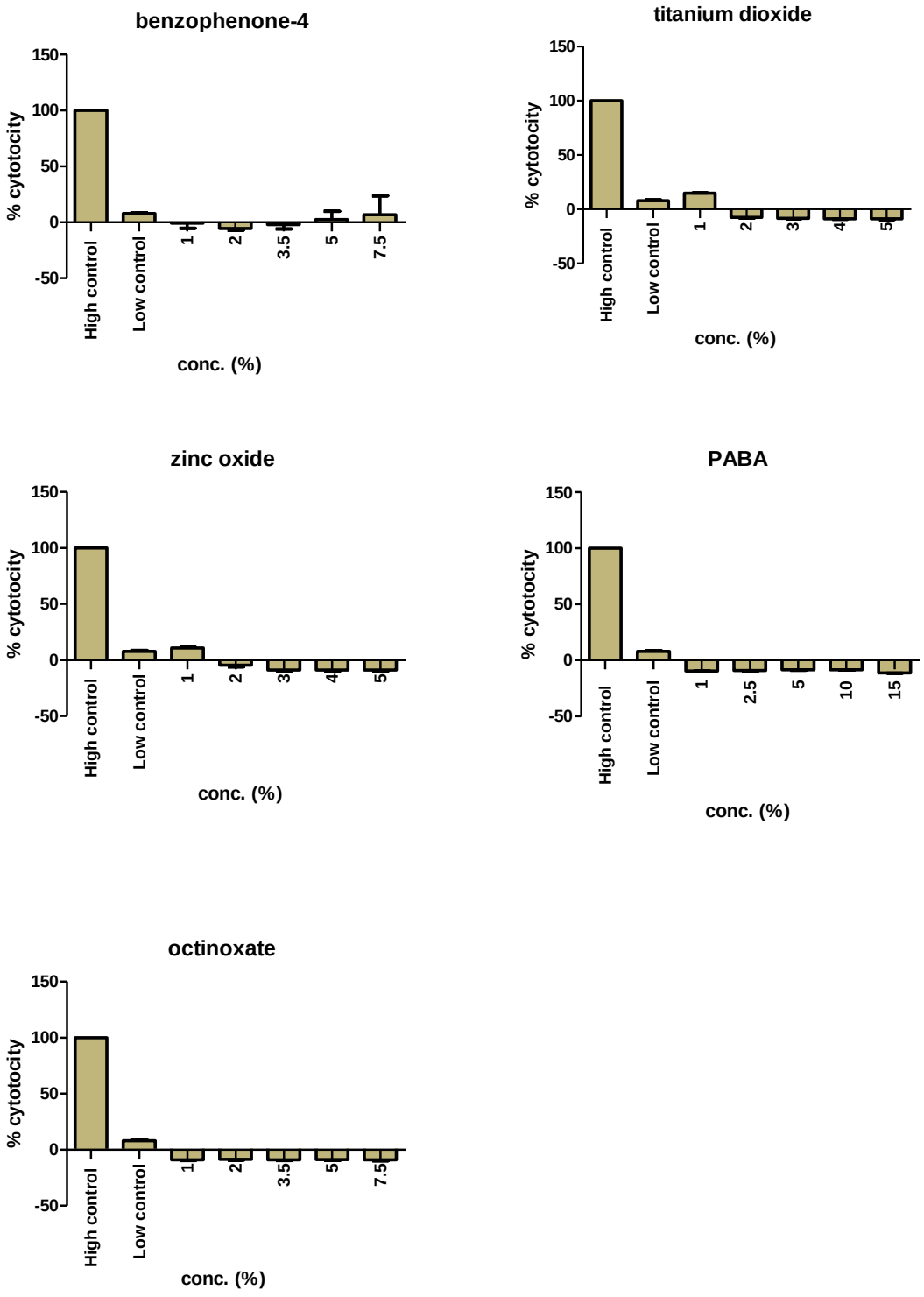

Figure 29 Graphs showing false negative results of the LDH cytotoxic assay, due to interferences by the sunscreen activies.

Appendix 6: Extracellular energy phenotype metabolic of the site-specific scalp fibroblast (discussion).

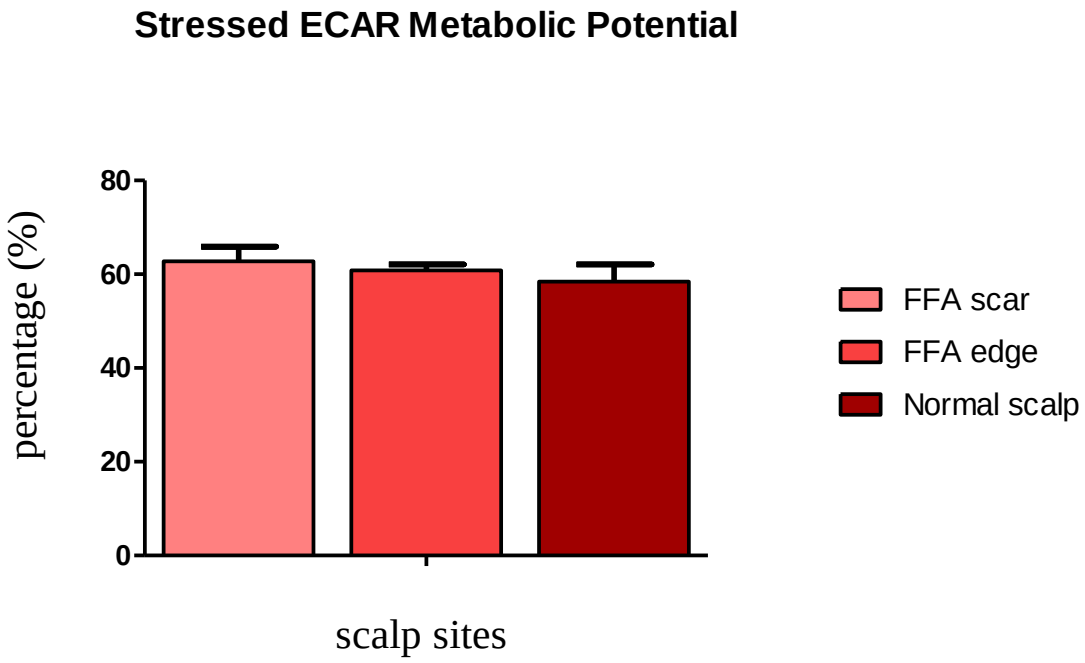

Figure 30 extracellular acidification rate of the untreated site-specific scalp fibroblasts.

Appendix 7: Patients' demographic data.

Table 10 Patient cosmetic history information given by the four FFA subjects whom were recruited for the study.

Participants	Gender	Age	Diagnosis year	Facial hyperpigmentation	Sunscreen use history	Medical history
P001	Female	61	2013	Yes	Occasionally	-
P002	Female	61	-	Yes	Started use after diagnosis	Sensitive skin, eczema
P003	Female	59	2004	Yes	Occasionally	Irritant contact dermatitis
P004	Female	55	2017	No	Yes	Hypertension